Phase-Locking Performance of Optical Injection-Locking Evaluated by Coherent Detection

For the degree of Master of Science

Martin Wahlsten

June 10, 2010

Department of Microtechnology and Nanoscience
CHALMERS UNIVERSITY OF TECHNOLOGY
Göteborg June 10, 2010

Abstract

The phase sensitive fiber optical amplifier (PS-FOPA), has shown potential for several key applications, for example extreme low noise amplification. Furthermore, PS-FOPAs implies strict demands of precise control of phase relations of the input optical waves to the amplifier. This phase-locking of optical waves can be done by utilizing injection-locking, which is a technique currently being used to some extent. In order to gain a deeper understanding of the phase-locking performance of injection-locking, novel coherent time domain measurements has been conducted. Performance measurements are focused on phase variance in time domain. The results agree with theoretical work previously done by Bordonalli et al. Several tradeoffs are identified, amongst them, between PM-to-PM transfer and AM-to-PM transfer. Balancing the injection ratio and locking-bandwidth for minimal phase noise is also concluded to be nontrivial.

Acknowledgments

Firstly I would like to thank my supervisors Peter Andrekson, and Carl Lundström for introducing me to and guiding me through such a stimulating and research focused thesis project close to the research done at the photonics laboratory. I am very grateful for the possibility to have experienced both interesting theory and a great deal of hands on approaches. I would also like to express my gratitude to Pontus Johannisson and Jörgen Bengtsson, two outstanding role models who always have time for questions and to enlighten the less brilliant. Doctor Zhi Tong also deserves special thanks for all the pointers in the lab and also for sharing his expertise on noise measurements. Many thanks also goes to PhD students and post-docs of the photonics laboratory who creates a stimulating and fun working environment, even at the most odd hours of the day.

My study companions at both master and bachelor levels should not go unnoticed, you know who you are, including Anders, Erik and Per.

My flatmates Markus and Olov deserves recognition for making life at home never dull nor lonely. Also I would like to thank my family for their long lasting support and faith in my abilities. Especially my brother, who has always been a guiding star.

Contents

List of Figures

List of Tables

1 Introduction

In recent research within the EU funded research project PHASORS, which aims to increase knowledge of phase sensitive parametric fiber amplifiers (PS-FOPA), needs regarding phase-locking of several optical waves has emerged. The fact that the parametric amplification process itself is highly sensitive to the relative phase of the incoming lightwaves to the PS-FOPA, is motivation enough to keep precise control of the relative phase. This precise control will henceforth be referred to as the process of phase-locking. The PS-FOPA is henceforth referred to as phase sensitive amplifier (PSA) and the phase insensitive fiber optical amplifier (PIA-FOPA) is denoted as PIA.

PHASORS has predicted and demonstrated several key applications for the PSA that cannot be realized with conventional amplifiers, for example the all optical regeneration of Binary Phase Shift Keying (BPSK) modulated data.

One existing technology for achieving phase locking is the process of injection-locking, schematically shown in figure 1. Conceptually injection-locking consists of two oscillators that can lock in frequency by injection of electromagnetic field, meaning that their relative phase difference will be static. These injection-locked oscillators were initially studied by Huygens who studied clocks and Adler who demonstrated, and evolved theories for injection locking in electronic circuits. Optical injection locking was demonstrated first by Stover and Steier 1966 [1], and was extensively researched during the 1980s as a base component for coherent communication.

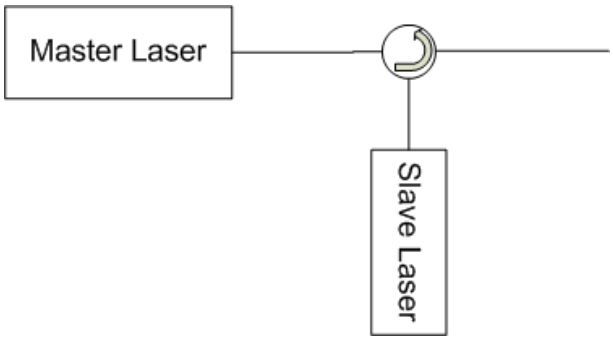

Figure 1: An injection-locked system, where the slave laser is forced to oscillate at the same frequency as the master laser, this due to the nonreciprocal coupling through the optical circulator.

As the interest in coherent communication diminished, with the rise of the rare-earth doped amplifiers, so did the interest in injection locking. The research was however revived in the years following the new millennium, mostly in the interest of examining the improved dynamics of an injection-locked laser. These enhanced dynamics allow higher direct modulation frequencies and is still of interest in low cost applications in optical communications [2]. Also recent research covers using injection-locked lasers for carrier regeneration, since its phase tracking characteristics together with amplification is desired.

This master thesis will focus on the potential of using injection-locking as a technology enabling the practical use of PSA:s and PSA related applications. This is analyzed using coherent measurements providing time domain information of the phase difference between the master laser and the slave laser.

The aim of the master thesis project is to design a measurement setup for coherent measurements, to identify phase tracking performance. Also desired is to identify system level performance tradeoffs, for systems that utilize injection-locking as a phase-locking technique.

1.1 Thesis Organization

The thesis, starts by motivating the necessity of phase-locking by describing four-photon mixing and phase sensitive amplification in section 2, for deeper understanding on background factors. An introduction to and the theory of injection-locking of lasers is presented in section 3. Section 4 briefly describes the current use of injection-locking together with PSA applications.

A scheme for exercising automatic control of detuning between master and slave lasers is introduced and explained in section 5.

The developed measurement system for coherent measurements is described is section 6. Section 7 describes the methods used and its limitations. The phase tracking performance is assessed in section 8, dominated by phase variance measured in different scenarios. Furthermore, the results are briefly discussed in section 9 and a set of conclusions are drawn in section 10.

2 Phase Sensitive Fiber Optical Parametric Amplifiers

The difference between PS-FOPA and the PI-FOPA, may at first glance be very small, however the differences for potential applications are very large. In common they share the parametric behavior which is based on nonlinear response of the polarization vector in the material [3]. In χ^3 processes, that is the dominating nonlinearity term for optical fibers, Four-Photon Mixing (FPM, also referred to as Four Wave Mixing (FWM)) is possible [3]. Other optical amplifiers like rare-earth doped fiber amplifiers, like the Erbium-Doped Fiber Amplifier (EDFA), and the Raman fiber amplifier relies on material energy transitions which amplifies the optical signal by stimulated emission. The FPM process rather amplifies by directly shifting optical energy from certain wavelengths known as the pump wavelengths to the signal wavelength, and to another wavelength called the idler wavelength.

One of the most exciting features of the PSA is its potential to approach very low noise figures. The noise figure is quantified as the Signal to Noise Ratio (SNR) at the input of the amplifier divided by the SNR at the output of the amplifier. For the EDFA, the Raman fiber amplifier, and the PI-FOPA there is an intrinsic limit to the noise figure that equals 3 dB [4]. However the phase sensitive parametric amplification process can approach a noise figure of 0 dB [5], which corresponds to noiseless amplification.

The possibility of near noiseless amplification is directly related to the ability of the PSA to amplify signal components with a certain phase.

The ability to squeeze the fluctuations in for example phase is the foundation for the ideas of all-optical in-line signal phase regeneration. A PSA can be used to translate phase jitter to amplitude jitter, and then the amplitude jitter can be decreased by saturated amplification. The phenomena of squeezed coherent states and can be assessed with the help of quantum mechanics as done by Levenson et al. [5].

2.1 Four-Photon Mixing

FPM is a nonlinear process that can occur in optical fibers, where four photons interact with each other while copropagating in a nonlinear medium. The wave representation of FPM denoted as FWM can physically explained by two waves beating in amplitude at their difference frequency, this beating induces changes in the refractive index in the fiber from its Kerr nonlinearity. The changes in the refractive index can in turn phase modulate a third wave at the difference frequency, producing sidebands. In turn the optical waves will beat with all other optical waves effectively phase modulating the remaining optical waves. Even though a plethora of optical frequencies will be created this way, only a few of the will build up and dominate the spectrum. These dominating waves are popularly referred to as pump(s), signal and idler as showed in figure 2. The same process can also be observed in a quantum mechanical way as the annihilation of two pump photons and the creation of a signal photon and an idler photon.

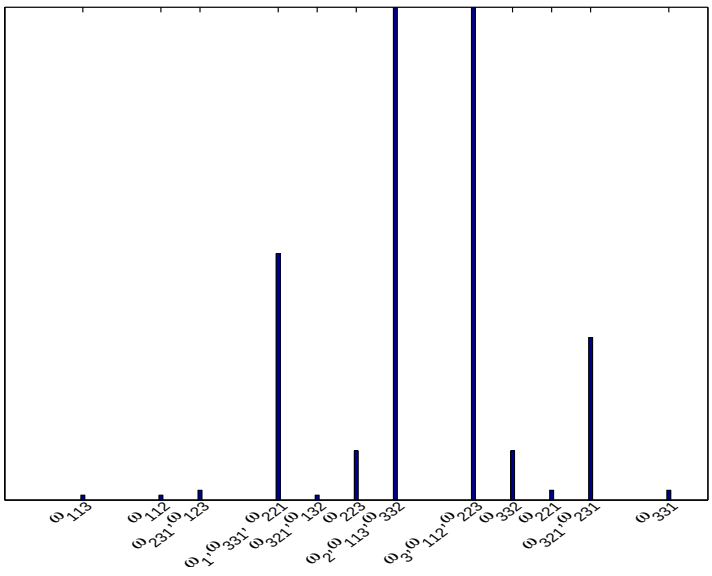

Figure 2: Frequencies generated by FPM, as a result from three input waves at ω_1,ω_2 and ω_3. [Figure adapted from [3]].

In figure 2, the four components dominating the spectra is ω_1 referred to as the signal, ω_2 and ω_3 are referred to as pumps. ω_{321} and ω_{321} constitutes the

idler generated in the FPM process [3]. The frequencies generated by FPM are denoted as $\omega_{k,m,l}$ where

$$\omega_{k,m,l} = \omega_k + \omega_m - \omega_l. \tag{1}$$

The nondegenerate FPM process is governed by two matching conditions where the four interacting photons conserving energy but allows a momentum mismatch. Let us now assume a process where two different pump photons at ω_{p1} and ω_{p2} amplifies a signal at the frequency ω_{signal} and generates an idler at ω_{idler}. Then these involved frequencies is bound by

$$\omega_{p1} + \omega_{p2} = \omega_{signal} + \omega_{idler}. \tag{2}$$

This condition effectively selects the idler frequency to one that will preserve the total energy in the system. Propagation constants of interacting photons can be mismatched, thereby allowing a mismatch in momentum , by assuming a nondegenerate case the propagation constant mismatch can written as:

$$\Delta\beta = -\beta_{signal} - \beta_{idler} + \beta_{p1} + \beta_{p2}. \tag{3}$$

By considering a degenerate case where $\omega_{p1} = \omega_{p2}$, which usually is the case in many applications of the FOPA, and assuming the electric field characterizing the pump, signal and idler. The assumed total electic field might be written as:

$$E(x,y,z) = f(x,y)A(z) = f(x,y)\frac{1}{2}[A_p(z)\exp(j\beta_0 p - j\omega_p t) +$$
$$+A_s(z)\exp(j\beta_s z - j\omega_s t) + A_j(z)\exp(j\beta i z - j\omega_i t) + \text{complex conjugates}]. \tag{4}$$

In equation 4, $f(x,y)$ is the modal distribution in the x-y plane, and $A_{p,s,i}$ is the slowly varying complex amplitude of the pump, signal and idler waves respectively. $\omega_{p,s,i}$ is the fundamental angular frequencies, $\beta_{p,s,i}$ is the propagation constants, of the pump, signal and idler waves. By inserting the total field into the nonlinear Schrödinger equation, also called the basic propagation equation, and neglecting fiber loss, it is possible to derive equations for the complex amplitudes $A_{p,s,i}$ [3],

$$\frac{\partial A_p}{\partial z} = j\gamma\left[(|A_p|^2 + 2(|A_s|^2 + |A_i|^2))A_p + 2A_s A_i A_p^* exp(j\Delta\beta z)\right] \tag{5}$$

$$\frac{\partial A_s}{\partial z} = j\gamma \left[(|A_s|^2 + 2(|A_i|^2 + |A_p|^2))A_s + A_p^2 A_i^* exp(-j\Delta\beta z) \right] \tag{6}$$

$$\frac{\partial A_i}{\partial z} = j\gamma \left[(|A_i|^2 + 2(|A_s|^2 + |A_p|^2))A_i + A_p^2 A_s^* exp(-j\Delta\beta z) \right]. \tag{7}$$

In equations 5 to 7, γ is the nonlinear coefficient of the material propagated in, and $A_{p,s,i}$ is the complex amplitudes of the pump, signal and idler electric fields respectively. $\Delta\beta$ is the propagation constant mismatch described in equation 3. In equations 5 to 7 several interesting terms arises, the first two terms is responsible for the nonlinear phase shifts. The first term is responsible for the self-induced nonlinear phase shift, called self phase modulation (SPM), while the second term is the nonlinear phase shift induced by the other waves, called cross phase modulation (XPM). The last term describes the flow of energy transferring between the optical waves.

The equations 5 to 7 can be rewritten to be described by powers and phases, according to [3], by letting $P_{p,s,i} = |A_{p,s,i}|^2$ and $A_{p,s,i} = \sqrt{P_{p,s,i}} \exp(j\theta_{p,s,i})$. Equations 5 to 7 then translates to

$$\frac{\partial P_p}{\partial z} = -4\gamma \sqrt{P_p^2 P_s P_i} \sin\phi \tag{8}$$

$$\frac{\partial P_s}{\partial z} = 2\gamma \sqrt{P_p^2 P_s P_i} \sin\phi \tag{9}$$

$$\frac{\partial P_i}{\partial z} = 2\gamma \sqrt{P_p^2 P_s P_i} \sin\phi \tag{10}$$

$$\frac{\partial \phi}{\partial z} = \Delta\beta + \gamma(2P_p - P_s - P_i) + \gamma \left[\sqrt{\frac{P_p^2 P_i}{P_s}} + \right.$$
$$\left. + \sqrt{\frac{P_p^2 P_i}{P_s}} - 4\sqrt{P_s P_i} \right] \cos\phi \tag{11}$$

$$\phi(z) = \Delta\beta z + 2\theta_p(z) - \theta_i(z) - \theta_s(z), \tag{12}$$

where ϕ denotes the phase difference between the optical waves, $P_{s,i,p}$ are the powers of the signal, idler and pump waves respectively. γ is the nonlinear

coefficient which is also a function of the effective modal area A_{eff}, on the form $\gamma = 2\pi n_2/(\lambda A_{eff})$, where n_2, is the linear dependence of the refractive index with respect to optical power per A_{eff}, and is measured in $\mathrm{m^2W^{-1}}$. Noteworthy is the $\theta_{s,i,p}(z)$ in equation 12 is the initial phase at $z = 0$ plus the acquired nonlinear phase shifts from propagation, $\Delta\beta$ is the dispersive shift linear with propagation distance. Also notable is the equation 12 is dependent on the parametric process assumed, here it describes the assumed pump photon degenerate case.

One of the most useful results that is clearly stated in the equations above is how the amplification process is phase dependent, so if all optical waves are present at the input the behavior of the amplifier can be tuned by their relative phases. From tuning this input phases, it is possible to achieve both amplification and attenuation of the signal, which is imperative for some of the anticipated applications of the PSA.

The phase dependance and the inherent ultrafast response time, on the femtosecond scale, allows the PSA to be used as an optical processing device on a real time bit to bit basis. The all-optical signal regenerator is an example where the PSA abilities of optical processing is utilized.

3 Injection Locking

Injection-locking is a technique where two lasers are nonreciprocally coupled and have a number of benefits. Light from a laser referred to as the master laser is coupled into the cavity of a secondary laser usually referred to as the slave laser. The power of the injected light is often small but can alter the behavior of the slave laser most dramatically. The injection-locking occur when the frequencies of the two lasers are sufficiently close to each other. The slave laser can then ***lock*** to the master laser efficiently locking the frequency of the light in the slave laser to the frequency of the injected light.

Injection-locking can improve the dynamics of the slave laser leading to a higher relaxation oscillation frequency, effectively allowing faster direct modulation of the slave laser [6]. The side mode suppression can also be enhanced in the slave laser when subjected to injection-locking [7]. Reduction in chirp and Relative Intensity Noise (RIN) of the directly modulated injection-locked slave laser is reported to be lower in several papers [8],[9], [10].

According to Pikovsky et al. [11] the first known formal observation of injection-locking was made by Christiaan Huygens, whom described this phenomenon in a letter to his father in 1665. Huygens observed how two pendulum clocks on the wall in his bedroom wall had a peculiar tendency to lock their relative phase to each other. Huygens argued for that these two clocks were coupled through the wall.

It was however not until Adler et al. started to injection-lock resonant electrical circuits that injection-locking was published the first time [12]. Adler showed that he could detune the electrical resonant circuit from it natural resonant frequency by injection-locking.

However, it was not until 1965 the theory of optical injection-locking was established by Pantell [13], [2], and the first demonstration of optical injection locking was performed by Stover and Steier in 1966 [1].

One of the key motivations behind this master thesis is to examine and provide knowledge on limitations and possibilities of the injection-locking technology as a enabling technologies for future PSA applications. Therefore a good insight into the basic mechanics of injection-locking is required.

3.1 Phasor Description of Injection-Locking

Injection-locking can be understood through a phasor representation of the normalized native and injected electric fields in the slave laser. The native laser field is in this subsection denoted as β and the injected field is referred to as $\Delta\beta$. Figure 3 shows a phasor representation of injection locking during the time Δt inside a slave laser with the round trip time of T. In figure 3 the coordinate system is defined such that the phase of the injected light always is zero, therefore ϕ denotes the phase difference between the master laser and slave laser.

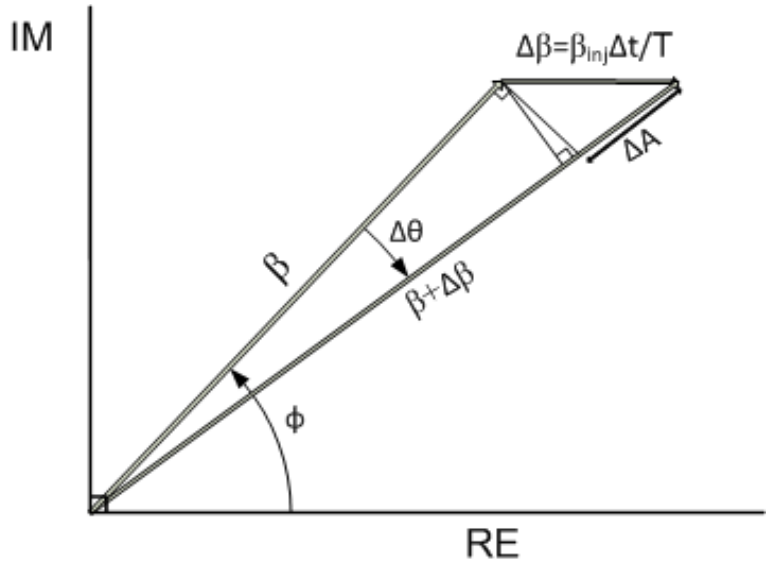

Figure 3: Phasor model over injection-locking during a short time Δt. [Figure adapted from [2]].

As Henry et al. [14] superbly explains there are two major effects making the two lasers to lock in frequency even though their cavities are detuned. Both of these effects can be understood from the phasor representation of injection-locking in figure 3.

The first, most evident effect, can be observed by realizing that the phase is changing with time, and since frequency is defined as $\frac{\partial \Delta\theta}{\partial\, t}$, frequency is shifted. The other effect comes from changing the resonance frequency in the cavity by altering the gain necessary to sustain lasing. The gain and tuning are coupled through the linewidth enhancement factor α.

It is possible to understand how the first effect can be quantified, by establishing how θ changes which can be described as:

$$\Delta\theta = -\arctan\frac{\sin(\Phi)\beta_{inj}\Delta t}{T\beta}. \tag{13}$$

Simplifications can be done in equation 13 by restricting the level of injected light to the regime where $\sin(\theta)\beta_{inj}\Delta t \ll T\beta$. The restrictive assumption is valid for most practical cases. Equation 13 can thereby be rewritten, by assuming that that the fields are normalized such that $I_{inj} = \beta_{inj}^2$, as:

$$\Delta\theta = -\sqrt{\frac{I_{inj}}{I}}\frac{\sin(\Phi)\Delta t}{T}. \tag{14}$$

By finding the phase progression as a function of time, the detuning of the coupled lasers through this effect can be found by a simple derivative, with respect to time, written as

$$\Delta\omega_1 \equiv \frac{\partial\Delta\theta}{\partial t} = -\sqrt{\frac{I_{inj}}{I}}\frac{\sin(\Phi)}{T}. \tag{15}$$

The second effect that detunes the slave laser involves how the gain changes with the injected light, and thereby detunes the cavity changing the refractive index via the linewidth enhancement factor. To understand the change in amplitude , ΔA which accounts for the change in amplitude can be written, according to figure 3, as:

$$\Delta A = \frac{\cos(\Phi)\beta_{inj}\delta t}{T}. \tag{16}$$

Then the change in intensity can be written as

$$\Delta I = 2|\beta + \Delta\ A|^2 - |\beta|^2 = 2|\Delta A\beta| + |\Delta\ A|^2. \tag{17}$$

By applying the condition of the low injection regime the approximation

$$\Delta I = 2|\Delta A\beta| + |\Delta\ A|^2 \approx 2|\Delta A\beta|, \tag{18}$$

can be made since $\beta \gg \Delta A \implies 2|\beta\Delta A| \gg |\Delta A|^2$. Substituting variables into equation 18 leads to

$$\Delta I = \frac{\sqrt{II_{inj}}}{T}\cos(\Phi)\Delta t. \tag{19}$$

However, in steady state ΔI is equal to zero so the gain dynamics has to make up for the change in intensity. During the time Δt, the gain dynamics must obey the following relation,

$$\Delta G = \frac{-\Delta I}{I \Delta t} = -2\sqrt{\frac{I_{inj}}{I}}\frac{\cos(\Phi)}{T}, \tag{20}$$

to compensate the output power during the time Δt [14]. In equation 20 ΔG is the change in cavity gain in terms of cm^{-1}. The acquired detuning due to gain altering can be expressed as:

$$\Delta\omega_2 = \frac{\alpha}{2}\Delta G = -\alpha\sqrt{\frac{I_{inj}}{I}}\frac{\cos(\Phi)}{T}. \tag{21}$$

The total detuning acquired can be found by addition of the two effects $\Delta\omega_1$ and $\Delta\omega_2$ forming

$$\Delta\omega_{tot} = -\sqrt{\frac{I_{inj}}{I}}\frac{1}{T}(\alpha\cos(\Phi) + \sin(\Phi)). \tag{22}$$

In conclusion, equation 22 gives a injection-locking bandwidth in which the $\Delta\omega_{tot}$ will negate the phase progression relative to the injected light forming a frequency locked system. This can be observed as a process described by figure 4 as previously done by Lau [2].

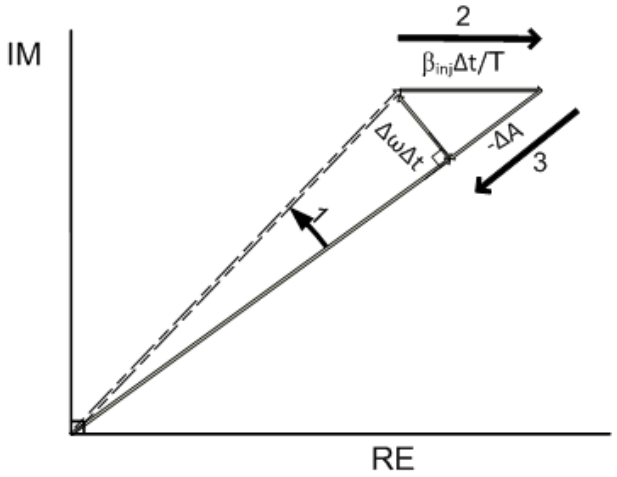

Figure 4: Phasor model over the injection-locked system's phase-locking properties. [Figure adapted from [2]].

In figure 4 three different effects are readily visible at any given small time Δt. These three mechanisms keep a constant phase relation between the master and the slave laser, effectively locking them in frequency. The different respect are represented by the numbered arrows in figure 4.

First, the detuning between the laser cavities tries to increase the phase difference with the linear phase progression term $\Delta\omega$.

Second, during the same time the injected light has influenced the phase difference between the laser light back to its original state.

Third, the amplitude of the field inside the laser falls back to the steady state value since the laser cannot sustain field amplitudes over the steady state value.

The phasor representation of injection-locking is powerful for intuitively understanding of some vital mechanics of injection-locking. However in order to gather deeper understanding and making numerical simulations, a more complete theoretical framework is presented by the rate equations.

3.2 Rate Equations

A model consisting of rate equations coupling the carrier population to the photon population in lasers is a well known, and well working model to describe most laser dynamics. The classical model based on rate equations nevertheless needs further modifications to include external injected fields. This in order to describe injection-locked systems. The model referred to in this thesis has been published by many different authors [14], [2], [15], [16] and [17].

Erwin Lau makes a very elegant derivation of these in [2], which starts with a differential equation for the electric field which in a laser can be written as:

$$\frac{\partial E(t)}{\partial t} = \frac{1}{2} g \Delta N(t)(1 + j\alpha)E(t) \tag{23}$$

$$\Delta N(t) \equiv N(t) - N_{threshold}. \tag{24}$$

In equations 23 and 24, E is the complex electric field, g is the linear unsaturated gain, $N(t)$ is the number of carriers, α is the linewidth enhancement factor. $\Delta N(t)$ is the number of carriers above the threshold carrier number $N_{threshold}$. The differential equation does not account for noise and spontaneous emission, as the laser is assumed to operate well over threshold, the spontaneous emitted contribution to the total field is negligible. However, a more serious limitation to equation 23 is that it does not take any outside field into account. Therefore equation 23 is suitably modified with two extra terms one to add the external field and one to account for the interaction between the two field components. The modified differential equation could then be written as:

$$\frac{\partial E(t)}{\partial t} = \frac{1}{2} g \Delta N(t)(1 + j\alpha)E(t) + \kappa A_{inj} - j\Delta\omega E(t) \tag{25}$$

$$\text{with } \Delta\omega \equiv \omega_{master} - \omega_{slave}, \tag{26}$$

where κ is the longitudinal mode spacing in Hertz for the slave laser, A_{inj} is the complex injected field directly after the input facet including coupling losses. The detuning between the two laser fields is denoted $\Delta\omega$ and is described by 26. ω_{master} refers to the angular frequency of the master laser electric field that gets injected in the slave laser which has an angular frequency of ω_{slave}. The third term in equation 25 describes the injection of the complex master laser field, and the forth term accounts for the beating that will arise from the different angular frequencies of the two fields.

It is now possible to make the identification $E(t) = A(t)\exp(j\phi(t))$, splitting up the complex field $E(t)$ in magnitude and phase, in equation 25. Finding three new coupled differential equations completes the set of coupled differential equations to describe the light injected system. These equations can be written as:

$$\frac{\partial A(t)}{\partial t} = \frac{1}{2} g \Delta N(t) A(t) + \kappa A_{inj} \cos\left(\Delta(t)\right) \tag{27}$$

$$\frac{\partial \theta_0(t)}{\partial t} = \frac{\alpha}{2} g \Delta N(t) - \kappa \frac{A_{inj}}{A(t)} \sin\left(\Delta(t)\right) \tag{28}$$

$$\frac{\partial N(t)}{\partial t} = J - \frac{N(t)}{\tau_{carrier}} - \left[\frac{1}{\tau_{photon}} + g[\Delta N(t)]\right] A(t)^2, \tag{29}$$

where J is the injected current normalized by the electron charge,$\tau_{carrier}$ is the carrier lifetime and τ_{photon} is the photon life time. $\Delta(t)$ is the phase

difference between the master laser field and the slave master field, which can be denoted as:

$$\Delta(t) = \Delta\omega(t) - \theta_0(t), \tag{30}$$

where $\Delta\omega(t)$ is the detuning between the master and the slave lasers and $\theta_0(t)$ is the phase shift induced by the injection-locking. Equations 27-29 is a versatile theoretical model that describes injection-locking.

3.2.1 Steady State Solutions to Rate Equations

In this subsection the steady state solutions is found to the theoretical framework provided by equations 27-29. Before solving any of the rate equations it is important to established a few features of the injection-locked systems. In steady state the phase difference between the lasers are stationary, therefore the injection-locking has to induce the a linear phase shift, such that the detuning between the lasers is canceled. The first basic equation describes the mentioned phase shift induced by injecting light in the steady state, which can be stated as:

$$\theta_0(t) = (\omega_{master} - \omega_{slave})t + \theta_{locked}, \tag{31}$$

where $\theta_0(t)$ denotes a time varying phase change induced by injection-locking, consisting of two terms when being in steady state. The first term compensates for the linear phase drift from the two lasers having different frequencies. Furthermore, the second term is a constant phase offset, decided by the detuning.

The concluding important insight is that an injection-locked pair of lasers in steady state oscillates at the same frequency effectively turning equations 30 and 31 into:

$$\Delta(t) = -\theta_{locked} = -\theta_{steadystate}. \tag{32}$$

From equation 29 a steady state solution for the injected carriers J can be found by realizing that the gain must be clamped in the non-injection-locked case in steady state which corresponds to $\Delta N = 0$ and also $\frac{\partial N(t)}{\partial t} = 0$. This makes equation 29 rewritable to:

$$J = \frac{A^2_{freerunning}}{\tau_{photon}} + \frac{n_{threshold}}{\tau_{carrier}}. \tag{33}$$

Where $A_{freerunning}$ is the field amplitude in the freerunning case and $n_{threshold}$ is the number of carriers required for transparency. If now equation 33 is inserted into equation 29 it is possible to find a steady state solution, which can be denoted as:

$$A^2_{steadystate} = \frac{A^2_{freerunning} - \frac{\tau_{photon}\Delta N_{steadystate}}{\tau_{carrier}}}{1 + \tau_{photon} g \Delta N_{steadystate}}. \tag{34}$$

A steady state solution for the number of carriers above threshold, $\Delta N_{steadystate}$, can be found directly from equation 27, by setting the differential to zero for steady state case. The steady state solution for $\Delta N_{steadystate}$ can then be written as:

$$\Delta N_{steadystate} = \frac{-2\kappa A_{inj} \cos\left(\theta_{steadystate}\right)}{g A_{steadystate}}. \tag{35}$$

The locked steady state solution, denoted as $\theta_{steadystate}$, is the relative steady state phase difference between the master laser and the slave laser according to equation 32.

More insight can also be achieved by investigating equation 28 and 31, by finding $\frac{\partial \theta_0(t)}{\partial t}$ in equation 31, not entirely surprising equation 31 transforms to:

$$\frac{\partial \theta_0(t)}{\partial t} = (\omega_{master} - \omega_{slave}). \tag{36}$$

Equation 36 can now be inserted into equation 28 to find

$$(\omega_{master} - \omega_{slave}) = \Delta\omega = -\kappa \frac{A_{inj}}{A_{steadystate}} (\alpha \cos\theta_{steadystate} + \sin\theta_{steadystate}). \tag{37}$$

The coupling between detuning between the lasers and the phase difference becomes evident in the locked steady state solution.

Finding the phase as a function of the detuning $\Delta\omega$ can be done by introducing, as done by Mogensen et al. in [17], $\Psi = \arctan(\alpha)$ then equation 37 can be written as:

$$\sin\left(\theta_{steadystate} + \Psi\right) = \frac{-\Delta\omega}{\kappa \frac{A_{inj}}{A_{steadystate}} \sqrt{1 + \alpha^2}}. \tag{38}$$

Mathematically equation 38 has the solution

$$\theta_{steadystate} = \left\{ \begin{array}{l} \arcsin \frac{-\Delta\omega}{\kappa \frac{A_{inj}}{A_{steadystate}} \sqrt{1+\alpha^2}} \\ \\ \pi - \arcsin \frac{-\Delta\omega}{\kappa \frac{A_{inj}}{A_{steadystate}} \sqrt{1+\alpha^2}} \end{array} \right\} - \Psi + p \cdot 2\pi,$$

where p is an integer. Furthermore, only one of these is valid, since the requirement for the laser to be stable, $N_{steadystate}$ has to be lower than $N_{threshold}$, effectively bounding $\Delta N_{steadystate}$ to negative values. Equation 35 is therefore bound to $\theta_{steadystate}$ to values on the interval $[-\frac{\pi}{2}, \frac{\pi}{2}]$. By realizing that the bottom solution to equation 38 can be discarded since it has can not produce physically time stable solutions, $\theta_{steadystate}$ can be written as:

$$\theta_{steadystate} = \arcsin\left(\frac{-\Delta\omega}{\kappa \frac{A_{inj}}{A_{steadystate}} \sqrt{1+\alpha^2}}\right) - \Psi. \tag{39}$$

Even more information can be extracted from the steady state solutions if equation 39 is considered together with the initial stability criterion $[-\frac{\pi}{2} \leqq \theta_{steadystate} \leqq \frac{\pi}{2}]$. It is then trivial to observe that $\theta_{steadystate}$ is bound to the interval

$$-\frac{\pi}{2} \leqq \theta_{steadystate} \leqq \frac{\pi}{2} - \arctan(\alpha) \tag{40}$$

Then equation 38, by inserting the limits found in equation 40, gives the locking bandwidth

$$-\kappa \frac{A_{inj}}{A_{steadystate}} \sqrt{1+\alpha^2} \leqq \Delta\omega \leqq \kappa \frac{A_{inj}}{A_{steadystate}}. \tag{41}$$

The asymmetric behavior of the injection-locking bandwidth becomes evident as the steady state locking-bandwidth is larger at the negative side of the detuning between the lasers.

Steady state analysis on its own is not good enough to provide all the information on whether the system is stably locked or not. Since small perturbations always will be present the initial locked state has to be self regenerative [2]. The stability of the injection-locked system will be further examined in the next section.

3.2.2 Small Signal Analysis of Rate Equations

In order to determine whether the lock between two lasers is stable or not, small signal analysis may be used to make sure that the system stay stable when subjected to small perturbations. The equations 27 to 29 are linearized around the stationary points found in the steady state analysis in chapter 3.2.1. And the following substitutions are made: $A(t) = A_{steadystate} + \delta A(t)$, $\theta(t) = \theta_{steadystate} + \delta\theta(t)$ and $N(t) = N_{steadystate} + \delta N(t)$. In order to do this analysis it is convenient to write the coupled system of equations on matrix form following the notation of Mogensen et al. [17],

$$\begin{bmatrix} \frac{\partial}{\partial t} + d_{11} & d_{12} & d_{13} \\ d_{21} & \frac{\partial}{\partial t} + d_{22} & d_{23} \\ d_{31} & d_{32} & \frac{\partial}{\partial t} + d_{33} \end{bmatrix} \begin{bmatrix} \delta A(t) \\ \delta\theta(t) \\ \delta N(t) \end{bmatrix} = \begin{bmatrix} F_{A(t)} \\ F_{\theta(t)} \\ F_{N(t)} \end{bmatrix}, \tag{42}$$

where

$$\begin{aligned} d_{11} &= -\tfrac{1}{2} g N_{steadystate} \\ d_{12} &= \kappa A_{inj} \sin(\theta_{steadystate}) \\ d_{13} &= -\tfrac{1}{2} g A_{steadystate} \\ d_{21} &= -\kappa \tfrac{A_{inj}}{A^2_{steadystate}} \sin(\theta_{steadystate}) \\ d_{22} &== \kappa \tfrac{A_{inj}}{A_{steadystate}} \cos(\theta_{steadystate}) \\ d_{23} &= -\tfrac{1}{2} \alpha g \\ d_{31} &= 2A_{steadystate}(\tfrac{1}{\tau_{photon}} + g N_{steadystate}) \\ d_{32} &= 0 \\ d_{33} &= \tfrac{1}{\tau_{carrier}} + A^2_{steadystate}. \end{aligned}$$

The $F_{A(t)}$, $F_{\theta(t)}$ and $F_{N(t)}$ can according to Mogensen et al. [17] be described as Langevin noise sources. According to Simpson et al. [18] the stabile locking region, is limited by the region of convergence of the dynamical system, described by the poles of the determinant of the leftmost system matrix in equation (42). The characteristic equation can be written in Laplace notation

as:

$$\begin{aligned} D(s) &= s^3 + s^2(d_{11} + d_{22} + d_{31}) + \\ &\quad + s(d_{11}d_{22} + d_{22}d_{33} + d_{33}d_{11} - d_{12}d_{21} - d_{13}d_{31}) + \\ &\quad + (d_{31}(d_{12}d_{23} - d_{13}d_{22})) + (d_{33}(d_{11}d_{22} - d_{12}d_{21})). \end{aligned} \tag{43}$$

The system is stable when the roots of the polynomial has negative real parts according to the Routh-Hurwitz stability criterion utilized in control theory [19]. Bear in mind though that linearization introduces uncertainties since higher order terms are neglected. Furthermore, the approximation is only valid with small offsets from the operating point. Therefore the Routh-Hurwitz stability criterion should be regarded as a necessary condition for stability but not a sufficient criterion.

3.3 Fundamental Noise Properties of Injection-Locking

The theory regarding noise properties will not be treated in full, but some relevant aspects and relevant results are described. The noise properties of the injection-locked systems has been studied thoroughly by Bondonalli et al. in [20], by developing a optical phase-lock loop representation of the injection locking, together with rate equations. Utilizing transfer function theory to deduce predictions of the phase variance of injection-locked systems.

Limitations to the phase-lock loop model of injection locking is that it does not include instability of the injection-locked system, impairing the use to stable regions. This is no limitation when working in the low injection ratio domain as done in this thesis.

The model used and proposed by Bondonalli et al. is shown in figure 5

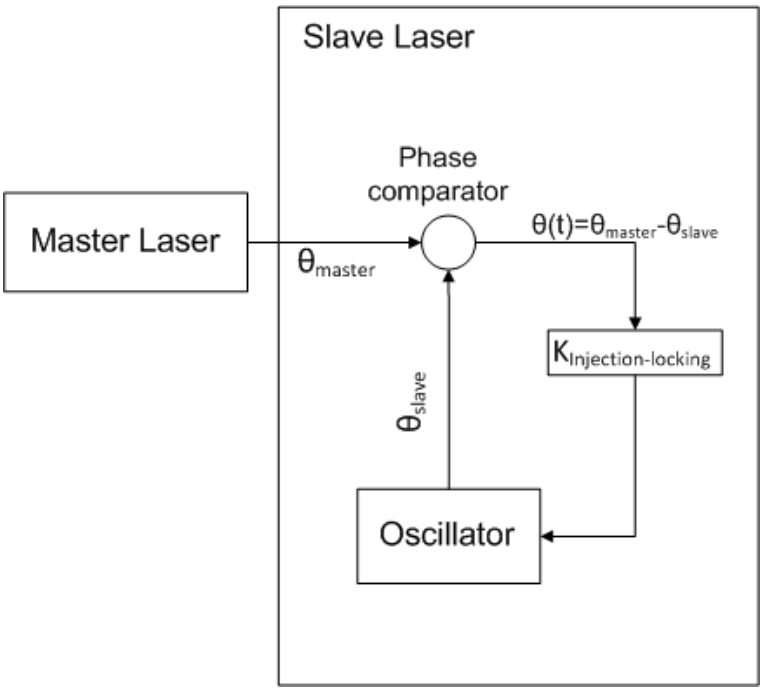

Figure 5: Model for a slave laser using phase-lock loop methodology. [Figure adapted from [20]].

The oscillator gets the feedback

$$\frac{\partial \theta_{slave}}{\partial t} = K_{Injection-locking}\theta(t), \tag{44}$$

making the oscillator to tune its frequency accordingly. The loop filter function is the $K_{Injection-locking}$ and is described by

$$K_{Injection-locking} = \frac{\partial \omega}{\partial \theta_{locked}} = \kappa\sqrt{\frac{P_{inj}}{P}}(\cos(\theta_{steadystate}) + \alpha \sin(\theta_{steadystate})), \tag{45}$$

where $\theta_{steadystate}$ is the fixed static state phase relation between the master and the slave laser, P_{inj} is the injected power into the slave laser, P is the optical power of the optical field inside the laser. Furthermore, κ is the longitudinal mode spacing and α is the linewidth enhancement factor.

For the system described in figure 5, after Laplace transformation, the transfer function can be deduced to

$$H(s) = \frac{K_{Injection-locking}}{s + K_{Injection-locking}}. \tag{46}$$

After a few approximations usually done when analyzing phase-lock loops, for further reading [20] is recommended, a spectral distribution of the phase error spectrum can be found, which can be written as:

$$S(f) = \left[\frac{FWHM_{master}}{2\pi f^2} + \frac{FWHM_{slave}}{2\pi f^2}\right] |1 - H(j2\pi f)|^2. \tag{47}$$

The theoretical results reflect how FWHM of the lasers impact the noise properties, even though the FWHM of the slave laser gets locked to the FWHM of the master in terms of linewidth. The inherent $FWHM_{slave}$ is still influencing the phase error spectrum.

Equation 47 is evaluated in figure 6, for different locked states where a difference in $\theta_{steadystate}$ corresponds to different detuning. Two different injection ratios is considered and and three different static phase differences to evaluate the phase noise power density spectrum.

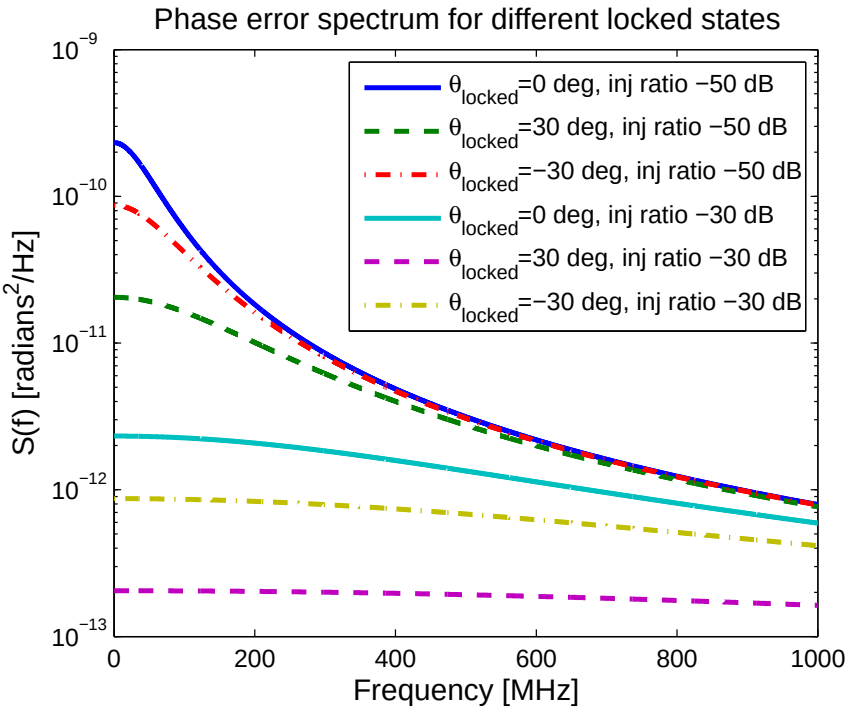

Figure 6: Phase error spectrum for two different injection ratios and three different static phase differences. The three topmost curves are results from the lower injection ratio while the three bottommost ones correspond to the higher injection ratio. Parameters that has been used are: summed laser linewidths 5 MHz, α=5, group index=4.3, effective cavity length 300 μm.

In figure 6 the three uppermost curves corresponds to different detunings at an injection ratio of -50 dB, while the three lower curves represents three different detunings at an injection ratio of -30 dB. Notable in the results is that different detunings at the same injection ratio yields different total noise power over the investigated bandwidth. This behavior is further studied in figure 20.

4 Current PSA Related Injection-Locking Applications

So far few papers that includes injection-locking as an enabling technology for PSA:s has been published due to the novelty of the ideas concerning this. However two interesting papers has so far been published within PHASORS, one by Weerasuriya et al. [21] and one by Parmigiani et al. [22].

Parmigiani et al. focuses on the first demonstration of a Differential Phase Shift Keying(DPSK) 40 Gbit/s regeneration scheme. This is implemented in an all-optical fashion and realizes one of the promises of the PSA. As showed in figure 7 the optical system includes an injection-locked slave laser. The role the of the slave laser in this setup is to lock onto the idler that arises from the PIA-process in the Highly Nonlinear Fiber (HNLF) 1. In this application it is vital that the locking-bandwidth is sufficiently small, such that carrier is recovered over a small bandwidth.

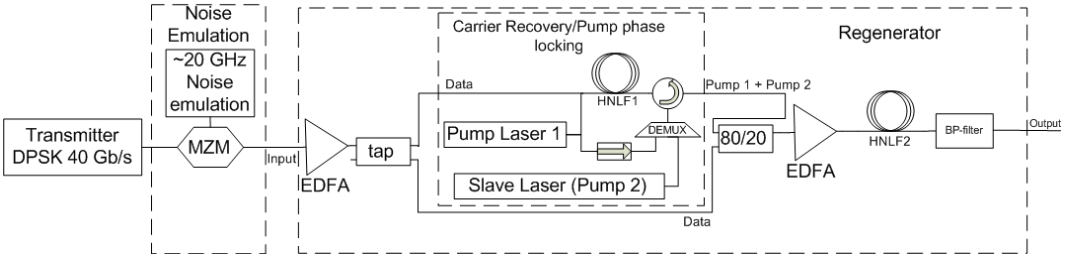

Figure 7: The schematic setup used by Parmigiani et al. for realizing the DPSK all-optical regenerator. [Figure adapted from [22]].

As shown in figure 7 the setup, is generating the three incident optical waves, that are required for the degenerate PSA, with a locked phase relation on the input of HNLF 2. This phase relation gives the highest gain for the two signal states 0 and π. Since both of these translates to the same idler phase in the PIA process in HNLF 1 according to Lu et al. [23], which is easily described as:

$$E_{idler} = \kappa A_{idler}^2 A_{pump} \exp(j\,((2\omega_{signal} - \omega_{pump})t + (2\phi_{signal} - \phi_{pump}))). \quad (48)$$

In equation 48, $A_{pump,signal}$ is the amplitude of the pump and signal waves, respectively. $\omega_{pump,signal}$ is in a similar fashion the angular frequencies for the

pump and signal wave. Finally the $\phi_{pump,signal}$ is the constant phase offset from a given reference for the pump and signal waves respectively. As seen if ϕ_{signal} only takes the discrete values 0 and π the modulation will not transfer to the idler wave since it will constantly be mapped to 0.

The generic noise added in the phase noise emulation step will be stripped away to large extent by the injection-locked slave laser. This because its locking-bandwidth is limited well under the approximately 20 GHz of phase noise emulation.

The second HNLF stage acts as a PSA effectively squeezing the phases towards the 0 and π of the signal state by providing phase dependent gain. The three optical waves that interact in HNLF2 is the signal that is tapped off at the side, the CW pump 1 and the modulation-stripped and noise-stripped idler from the PIA-stage in HNLF 1 after injection-locking.

The other paper that is published in the PHASORS project is work by Weerasuriya et al. [21], who use injection-locking to generate the input waves to a PSA for the BPSK signal format. The basic idea and realization is very similar to the work of Parmigiani et al. A PIA is used to create a idler which acts has a carrier for the BPSK signal since the modulation is stripped away as described by equation 48. The carrier is then used to injection-lock a discrete mode semiconductor laser. The system provides the necessary input phase-locked waves for signal-idler degenenerate phase sensitive amplification for the BPSK format.

The application involving injection-locking are dual pump and signal-idler degenerate, making it wavelength division multiplexing incompatible. Current PSA realizations done are not transparent in terms of modulation formats, which impedes their usability and scalability in the anticipated increased complexity of modulation format. Especially as Lu et al. anticipates that in the future all optical network several different modulation formats would coexist [23].

As explained in previous paragraphs the current injection-locked systems used together with PSA:s are dependent on small locking-bandwidths. This since the carrier should be as spectrally pure as possible to enhance the PSA processes, providing squeezed states and/or gain. The small locking-bandwidth puts strict demands on the drifts of the preferred cavity mode of both the lasers used, this since approaching and reaching unlocked states results in severe degradations in phase-locking performance.

5 Control of the Injection-Locking Process

To successfully build and implement systems with injection-locked solutions with very small locking bandwidth (hundreds of MHz) automatic control of detuning is needed to keep the lasers locked. Small locking bandwidth is a figure of merit in the application of injection-locking that was described in section 4. The small locking-bandwidth would make injection-locked slave lasers more resistant against phase modulation transfer.

A small locking-bandwidth would require a small injection ratio since the bandwidth scales with injection ratio according to equation 41. This in turn puts strict demands on laser drifts in both master and slave lasers, since those are not allowed to deviate from the locking-bandwidth. Deviating from the locking-bandwidth would make the lasers unlock and make the relative phase random. Therefore, it would be desirable to monitor the locked laser pair, and gain information on detuning between them, in order to enable active control of the detuning.

Pezeshki et al. [24] demonstrates a control scheme based on the study of the Modulation Transfer Ratio(MTR). The master laser gets amplitude modulated with an external Mach-Zehnder Modulator(MZM), and the modulation after the slave laser is monitored in order to find the MTR. MTR is defined as:

$$MTR = \frac{\Delta E_{slave}/E_{slave}}{\Delta E_{master}/E_{master}}. \tag{49}$$

In equation 49, $E_{master,slave}$ is the field amplitudes for the output of the master and slave laser respectively and $\Delta E_{master,slave}$ is the amplitude of the of the perbutation of the field amplitudes induced by the amplitude modulation. By conducting rate equation analysis including including modulation and assuming a discrete mode DFB laser, an analytical expression for the MTR can, according to [24], be written as:

$$MTR = \frac{1}{1 + \frac{K}{\tau_{photon}\kappa}\frac{P_{slave}}{P_{sat}+P_{slave}}\sqrt{\frac{P_{slave}}{P_{master}}}\sqrt{1 - \left(\frac{\Delta\omega}{\kappa}\right)\frac{P_{slave}}{P_{master}}}}. \tag{50}$$

When calculating the MTR, K is a constant which can be described as the ratio of roundtrip gain divided with the roundtrip loss in steady state, τ_{photon} is the photon lifetime, and κ is the longitudinal mode spacing in Hertz. $P_{slave,master}$ is the optical output power of the slave laser and the injected

power from the master laser respectively. Finally, P_{sat} is the saturation output power of the slave laser.

In equation 50 it is clearly visible that the lowest MTR is obtained when the detuning $\Delta\omega$ is zero. This fact is used by Pezeshki et al. [24] and is a feasible way to do detuning tracking. Figure 8 is a plot over equation 50 for some different injection powers and detuning frequencies. Notable from figure 8 is the distinct U-shaped curves with edges coinciding with the locking-bandwidth. Together with the fact that the minima of MTR coincides with zero detuning makes MTR a good candidate to be used for active control of the detuning.

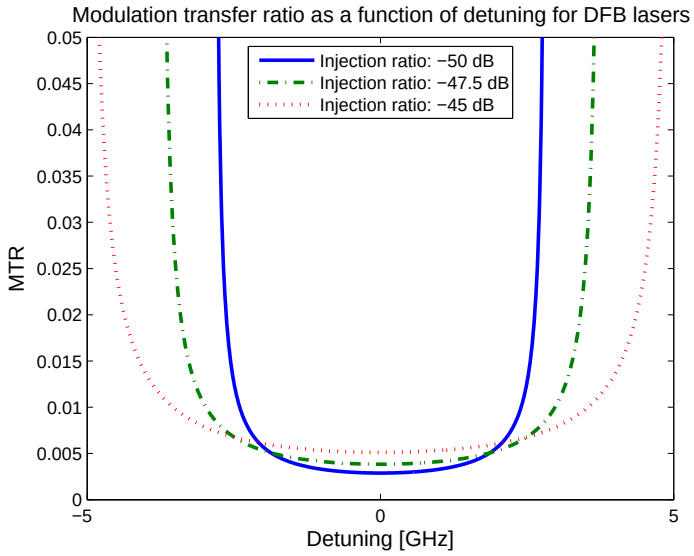

Figure 8: MTR as a function of detuning, parameters used are κ =142.85 GHz, K =1000, P_{sat} =1 mW and P_{slave} =1 mW.

Even though MTR is very small it can be measured with lock-in techniques. The basic idea behind the control loop is to measure the MTR with a lock-in amplifier and dither the MTR using a second tone to keep the MTR at minima since it coincide with zero detuning.

A control system for tracking detuning proposed and implemented by Pezeshki et al. [24] is schematically depicted in figure 9.

The MTR can be readily measured by lock-in amplifier 1 in figure 9, however the error signal needs to be the derivative of the MTR curve. This in order

to find the correct direction of detuning for active tuning of the slave laser current and thereby its frequency. The solution for finding the derivative implemented by Pezeshki et al. [24], consists of a second dithering tone introduced to the current controller. By dithering the MTR detected by the first lock-in amplifier, a second lock-in amplifier with the second tone as a reference finds the derivative of the MTR curve. Finally digital threshold and counter circuits provides feedback to the slave laser controller, to minimize the magnitude of the derivative of the MTR curve.

Before the slave laser also a light modulator has to be inserted together with a signal driver for the modulator. The signal driver also provides the reference signal for lock-in amplifier 1.

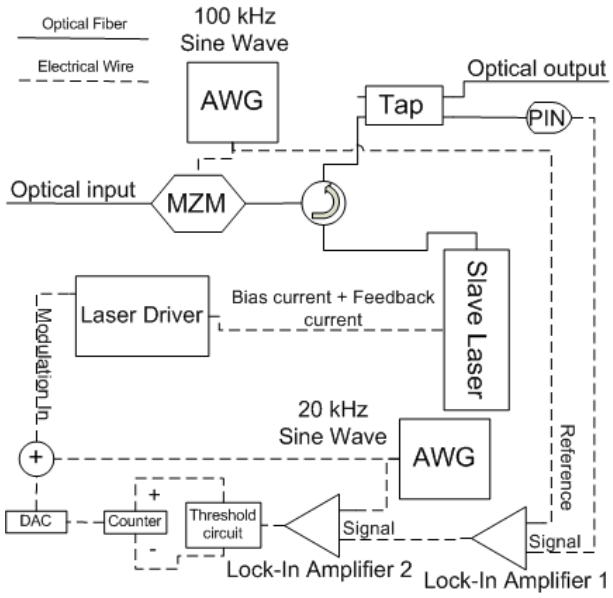

Figure 9: A setup for controlling the detuning between injection-locked lasers, where AWG stands for Arbitrary Waveform Generator, AOM for Acusto-Optic Modulator and DAC for Digital to Analogue Converter. [Figure adapted from [24]].

The total system complexity is of course considerably higher if such a control system is needed to achieve sufficient stability, such that the system can remain locked over time. Other drawbacks comes with the necessity of tapping some useful signal off for the control purpose and the amplitude to phase modulation transfer.

6 Measurement System Setup

In order to evaluate the future possibilities of optical injection locked systems, a measurement setup has been developed for determining several key performance parameters. The measurement system utilizes coherent detection in order to assess the phase tracking performance in time domain.

In figure 10 the optical setup used for the measurements of the phase tracking performance is depicted. The master laser used is a Santec TSL210 tunable laser with a linewidth of 800 kHz in the 1550 nm region. The slave laser used is a JDSU CQF935/5617.5 DFB laser with a specified linewidth below 1 MHz, and a wavelength of 1542.94 nm.

The hybrid used is polarization state sensitive and the polarization of both local oscillator input and signal input needs optimization before entering the hybrid. The hybrid then effectively has one optical output for the in-phase and one for the quadrature, which gets converted into electrical signals by a pair of matched detectors. The output is then sampled by a real time oscilloscope. The oscilloscope used is the Lecroy Wavemaster 8300, at a sample rate of 20 GS/s, and an analogue bandwidth of 3 GHz.

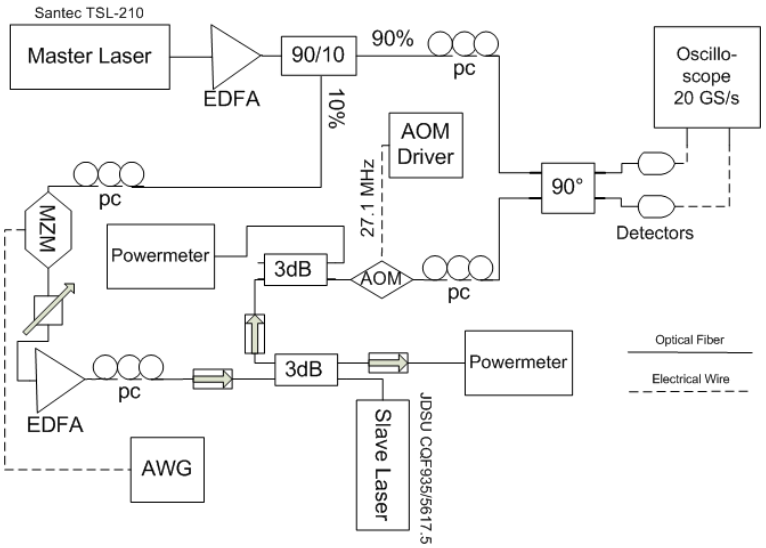

Figure 10: The basic optical setup used to measure phase-locking performance of the injection-locked system in time domain, where AWG stands for Arbitrary Waveform Generator and AOM stand for Acusto-Optic Modulator.

The upper arm of the interferometric setup can be called the local oscillator(LO) arm, because it provides the coherent reference for the coherent detection. The other arm can be treated as the signal arm since it is expected that the injection-locking process would introduce phase noise. The acusto-optic modulator (AOM) in the signal arm is fed with a 27.1 MHz sine tone, in order to make the scheme heterodyne to be compatible with the DC-blocked detectors used.

No intermediate frequency tracking has been implemented in software. The only software processing done on the samples is the substraction of the linear phase progression of the 27.1 MHz, corresponding to the AOM frequency in the signal arm.

6.1 Hardware Limits of the Measurement System

The initial studies of injection locking was made with a Mitsubishi FU-65SDF, an uncooled DFB laser. Experience using the Mitsubishi laser, showed that the short term drifts in preferred cavity mode was to large and to fast, to reach a small locking-bandwidths and also a lot of measurements became unrealible. A measure on stability is to let the two lasers freerunningly be detected by acoherent receiver and calculate the difference frequency with the help of linear regression of the phase. The short term drift between the lasers was estimated to $\pm$ 25 MHz.

Another fundamental limitation is how good the detuning can be set between the lasers using either temperature or current to tune the slave or master laser cavities. The most sensitive and continuous tuning for this setup was achieved with using the slave current source for tuning.

Optical isolation of the JDSU slave laser used in the experiments severely limits the dynamical range on injection ratios that is possible to reach. The range in terms of external injection ratio were locking was achieved was between -55 and -30 dB. Also, the uncertainty in the absolute external injection ratios are high since the isolation of the JDSU laser is not known, a minimum of 30 dB, and a typical value of 35 dB is specified in datasheet.

7 Measurement Methodology

Phase variance has been selected as a measure of phase tracking performance since variance is a measure on how much a stochastic variable varies around a its mean value. The results of a phase variance measurement can vary quite drastically both as a function of time and as a function of the number of consecutive samples used to calculate variance. Therefore, in the measurements undertaken, if nothing else is stated all phase variance measurements is done by concatenating 10 different batches measured over 250 ns to achieve an averaging effect.

Table 1 shows key equipment used which has significant impact on measurements.

Table 1: Equipment used

Equipment used	Model
Master Laser	Santec TSL-210
Slave Laser	JDSU CQF935/5617.5
Optical Spectrum Analyzer	ANDO AQ 6317B
Oscilloscope	Lecroy Wavemaster 3000
Photodetectors	Nortel PP-10G

The Lecroy Wavemaster 3000 used has an analogue bandwidth of 3 GHz, which serves as the limiting noise bandwidth for measurement system. In the most cases a majority of the phase noise power lies well within this bandwidth, as shown in figure 6.

During the measurements the OSNR of the signal used to injection-lock the slave laser is, if nothing else explicitly stated, 44 dB.

The powers measured being injected to the slave laser includes the ASE spectrum from the two EDFA:s. This in order to maximize the available dynamic range of the system unfortunately at a minor cost of external injection ratio measurement accuracy.

7.1 Sensitivity and Accuracy

Performance in term of sensitivity, the smallest phase variance that is possible to measure, has been measured with an simplified setup. The measurement setup was modified for determining the sensitivity of the measurement setup itself without any influence of the injection-locking. Figure 11 shows the setup used for noise floor measurements.

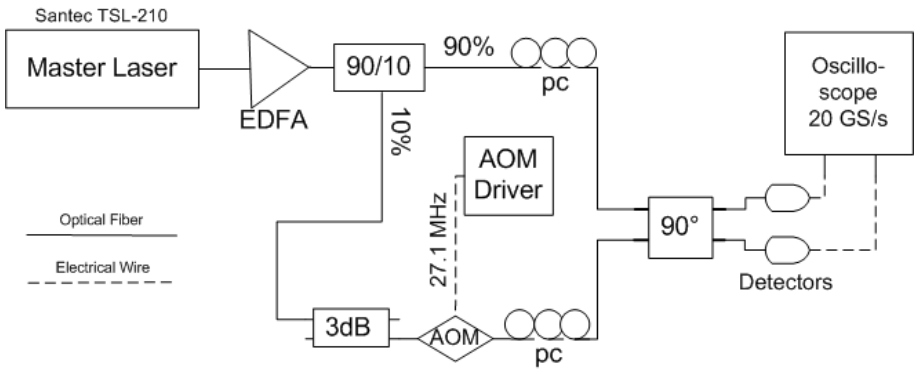

Figure 11: The measurement setup used for determine the noise floor of the phase variance measurements.

The altered setup should provide information about the smallest possible measurable phase variances. The LO arm and the signal arm of the interferometric setup are now unaffected by the injection-locked process. Phase noise from the AOM, and path length mismatch is believed to dominate the phase variance.

Memory depth is a crucial parameter when measuring phase variance, since a too short measurement time would yield statistically uncertain variances while a to long would start to include phase fluctuations unrelated to injection-locking. Phase fluctuations that onsets over long measurement times is for example AOM frequency uncertainty.

Figure 12 shows the results of a study of phase variance and memory depth, conducted with the reduced setup, described by figure 11. It compares the method used, concatenation of 10 batches of 5000 samples, and averaging the variance over 10 different very long measurements at different memory depths. The variance is calculated on all previous samples up to the current

number of samples on the x-axis. The 95 percent confidence intervals were found and shows that the measurement uncertainty is about ± 0.6 mrad^2.

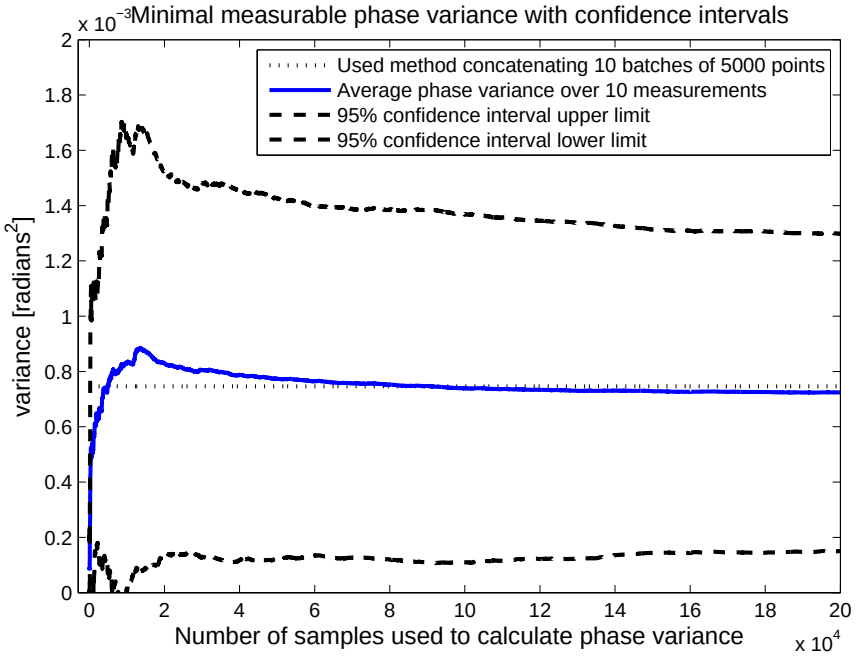

Figure 12: A reference method plotted with 95% confidence intervals as comparison to the variance measurement method used. The reference is consisting of the average of 10 different phase variance measurements, the variance is individually calculated as a function of memory depth before averaging.

The systematic rise that peaks around 10K samples, correlating to period time of a wave with a frequency of 1 MHz, is believed to be due the linewidth of the master laser. Since no path length matching has been undertaken, the linewidth of the master laser would be interpreted as phase variance. During longer measurements the laser has time to slightly change its frequency during the small delay in propagation time. Furthermore, the dynamics of the frequency changes are governed by the linewidth, so it takes certain time before this effect manifests, as seen in figure 12.

The method of collecting ten measurements consisting of 5K samples each also seem to get quite close to the mean phase variance over 200K samples.

7.2 External Injection Ratio

The injection ratio is an important parameter since it governs the physical processes of injection-locking. Unfortunately this parameter is truly inaccessible for direct measurements since it involves field amplitudes inside the slave laser. The injection ratio is defined as

$$\left(\frac{A_{injected}}{A}\right)^2 = \frac{P_{injected}}{P}, \tag{51}$$

where $A_{injected}$ is the field amplitude of the injected light after coupling into the laser and A is the amplitude of the field already existing in the laser. Since the field amplitudes inside the laser is inaccessible, external injection ratio can be used. External injection ratio a measurable quantity that is related to the injection ratio as described by Lau [2]. The external injection ratio is defined as:

$$\frac{P_{injected,outside}}{P_{out}}, \tag{52}$$

where $P_{injected,outside}$ is the measured power at the input facet of the slave laser, while P_{out} is the output power of the slave laser.

The external injection ratio scales as the injection ratio does since they are related by a constant, the constant can be derived considering traveling waves inside the laser, as done by Lau [2], the constant can be quantified as:

$$\frac{\text{Injection ratio}}{\text{External injection ratio}} = \frac{(1-r)^2}{r}. \tag{53}$$

The amplitude reflectivity of the laser mirrors, denoted r, is here assumed to be symmetrical at both ends of the laser used.

8 Measurements of the Performance of the Injection-Locking Process

The measurements done on the injection locked slave laser is primarily phase variance measurements since phase tracking is a key parameter for the PSA related applications. Also, RIN performance of the injection-locked pair has been assessed. However, the first object of interest is in which states the slave laser is lockable in terms of external injection ratio and detuning.

8.1 Locking Map and Locking Bandwidth

In order to increase the general knowledge and experience around injection-locking, the locking map was measured with the help of the real time oscilloscope, visually observing the limits of the locking-bandwidth. Also, the detuning of the lasers was measured with the same oscilloscope by breaking the coupling between lasers. The resulting map over lockable states is presented in figure 13.

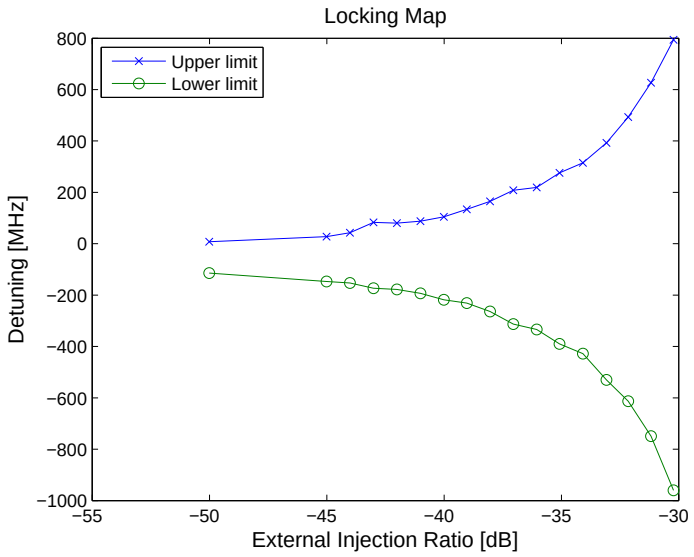

Figure 13: Locking map showing two detuning limits, which limits the states where locking was achieved.

Notable in figure 13 is the asymmetry in the upper and lower limits in the locking bandwidth, this because of a nonzero α-parameter seen in equation 41. Figure 14 shows the stable locking bandwidth as a function of the external injection ratio, notable is the linear relationship between the external injection ratio which is not expected. Expected behavior according to equation 41 linearly growing with the field amplitude rather than the power. Essentially the locking bandwidth should scale linearly with the square root of the injected power.

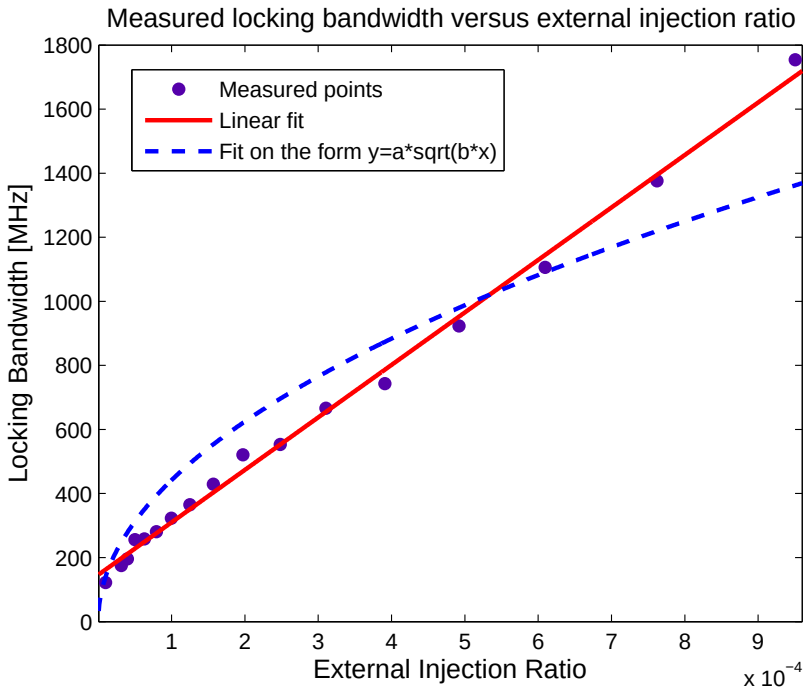

Figure 14: Observed locking bandwidth as a function of external injection ratio. Two functions are fitted to the data, one 1st grade polynomial and a function on the form y=a$\cdot\sqrt{b \cdot x}$, where a and b are constants.

As evident in figure 14 the measured locking bandwidth has a tendency to fit to the y=a$\cdot\sqrt{b \cdot x}$ function at low injection ratios but rather quickly diverge. The results of this measurements could have had decreased accuracy due to the method used. Visually observing the sampling scope to decide when the lasers were locked is a rather subjective measure. Another source of inaccuracy could stem from the high input power to the slave laser altering its parameters by inducing heat.

8.2 Phase-Locking Performance

The phase tracking performance of injection-locking has been evaluated with the help of the measurement setup described in figure 10. Both the intrinsic properties and provoked scenarios of the phase tracking performance has been evaluated. Provoked scenarios consisting of dithering tones in both amplitude and phase has been introduced. Also a brief study on how the Optical Signal-to-Noise Ratio (OSNR) influences the phase tracking performance. These are all important aspects of practically using injection-locked subsystems in PSA applications.

Since the master laser is also used as the LO reference for the coherent receiver the ideal result of the phase tracking performance measurements would be a collapsed dot in signal space having no variance in angle. Figure 15 shows the signal space of two unlocked lasers approximately 400 MHz detuned from each other as a comparison to the constellation diagrams gathered in different locked states in figure 16.

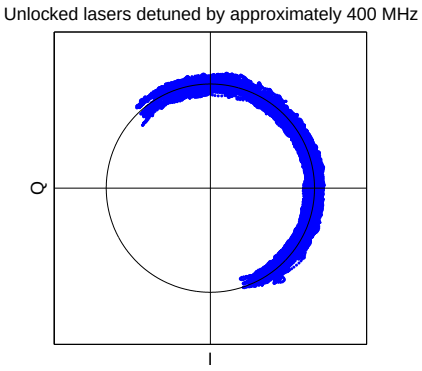

Figure 15: Signal space representations of 10 overlapping measurements during 250 ns without injecting any optical power, lasers detuned approximately 400 MHz.

Since no intermediate frequency recovery is done, the phase drifts between the two unlocked lasers in figure 15. The drift does not cover entire signal space since 10 measurements over 250 ns is combined to form the raw data, each measurement does not have the required time to cover the full range of phases. This would been the case if the detuning frequency been higher or the measurement time longer.

Figure 16 shows phase variance over a series of different external injection ratios using injection-locked lasers. Notable is the visual trend of more extended phase variations as the external injection ratio assumes smaller values as described by Bordonalli et al. [20].

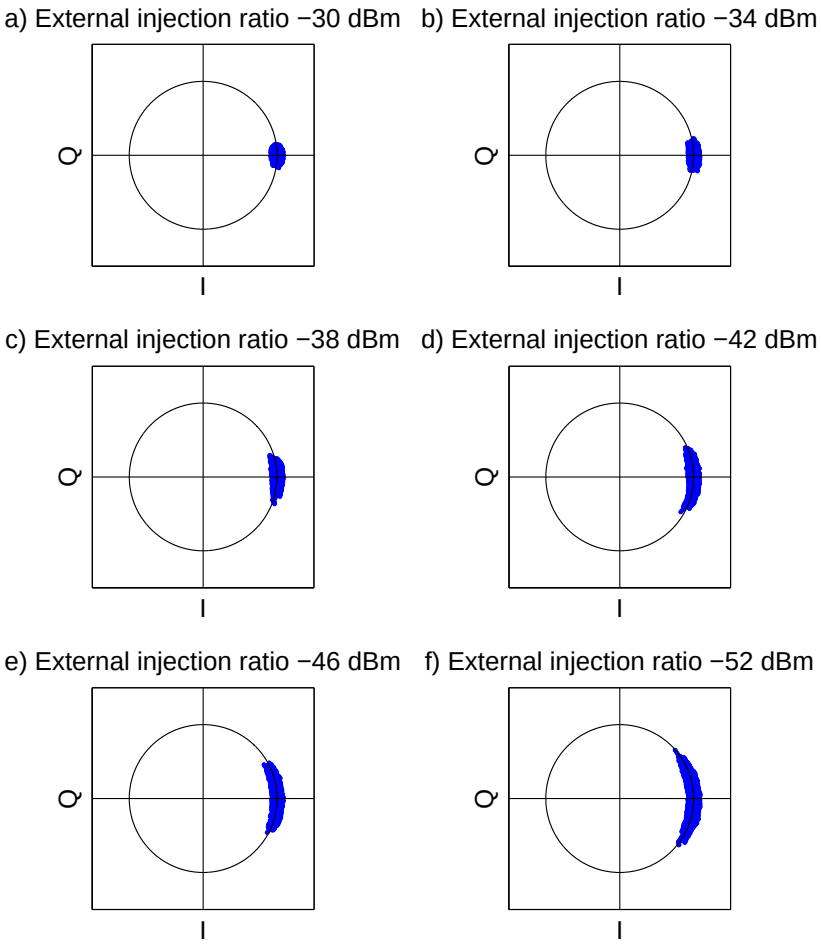

Figure 16: Complex plane representations of measurements with different external injection ratios, while keeping lasers at approximately zero detuning. Each signal space representation consists of 10 concatenated measurements each over 250 ns.

The measured constellation diagrams has also been studied from finding the phase variances of different external injection ratios as shown in figure 17.

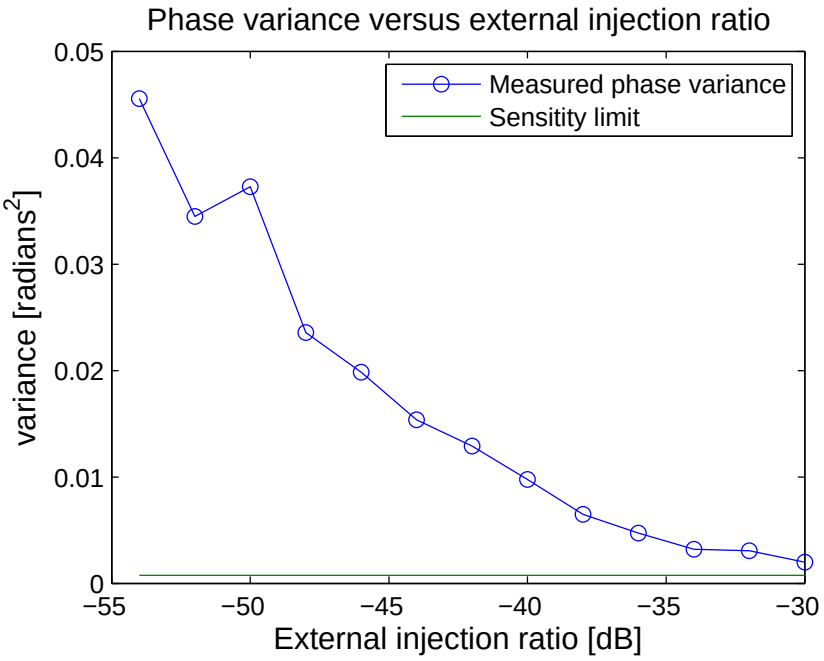

Figure 17: Phase variance as a function of external injection ratio. The locked measurements conducted at close to zero detuning and an OSNR of 44 dB. Also, the constant measured sensitivity limit of 0.75 mrad^2 is plotted for comparison.

The results clearly shows that there is a penalty to decreasing the injection-ratio trying to reach smaller injection ratios. One source of the additional phase variance stems from equation 39, showing how the static phase relation relates to detuning. The sensitivity, for changes in $\Delta\omega$, scales inversely with the injection ratio. This if the fluctuations of the detuning is constant disregarding of the injection ratio.

The variance increase observed in figures 17 and 16, can also be observed by studying the Probability Density Functions (PDF:s). Finding time information of the signals allows finding for example the PDF:s of the signals in phase to enable further mathematical treatment and methods to analysis. The PDF of the phase of three measurements done at different external injection ratios are shown in figure 18.

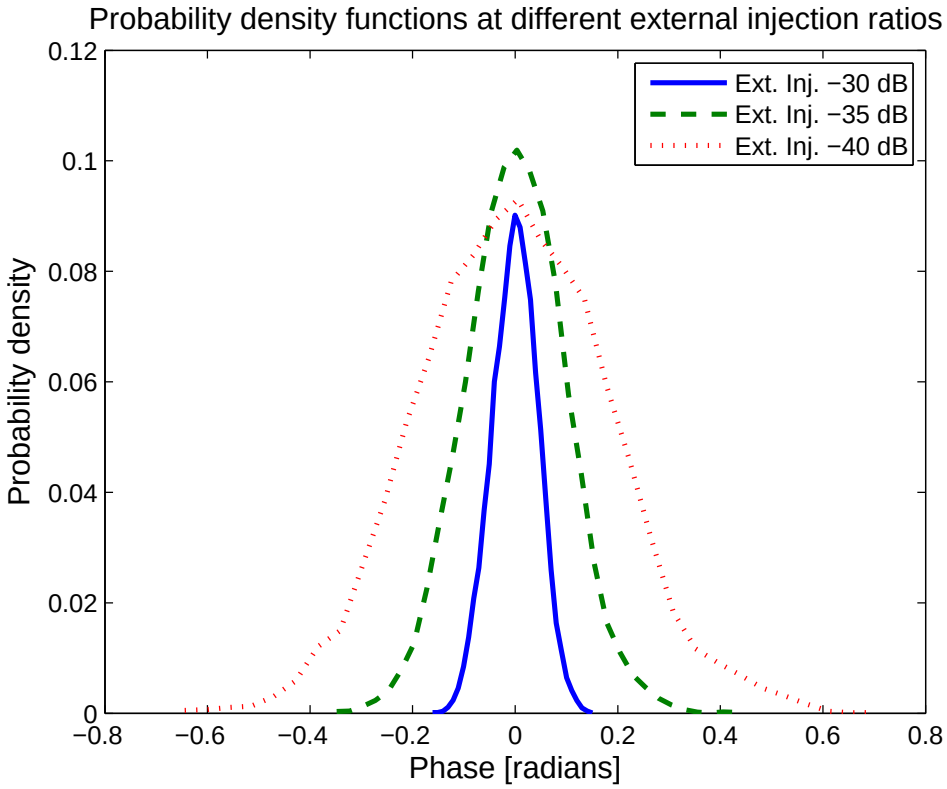

Figure 18: Phase PDFs for different external injection ratio. The locked measurements conducted at close to zero detuning.

In figure 18 the PDF is found by using 64 bins histograms for smoothing reasons. The gaussian shape of the data is quite evident for all three PDF:s. This information can be used for example to calculate linewidth, as done by Duthel in [25].

In comparison to altering the external injection ratio, a study of phase variance dependence on OSNR was conducted and presented in figure 19. To achieve the different OSNR the variable optical attenuator, situated after the MZM in figure 10 was used to attenuate the signal before the last EDFA stage. The OSNR was measured by the input of the slave laser with an ANDO AQ 6317B optical spectrum analyzer.

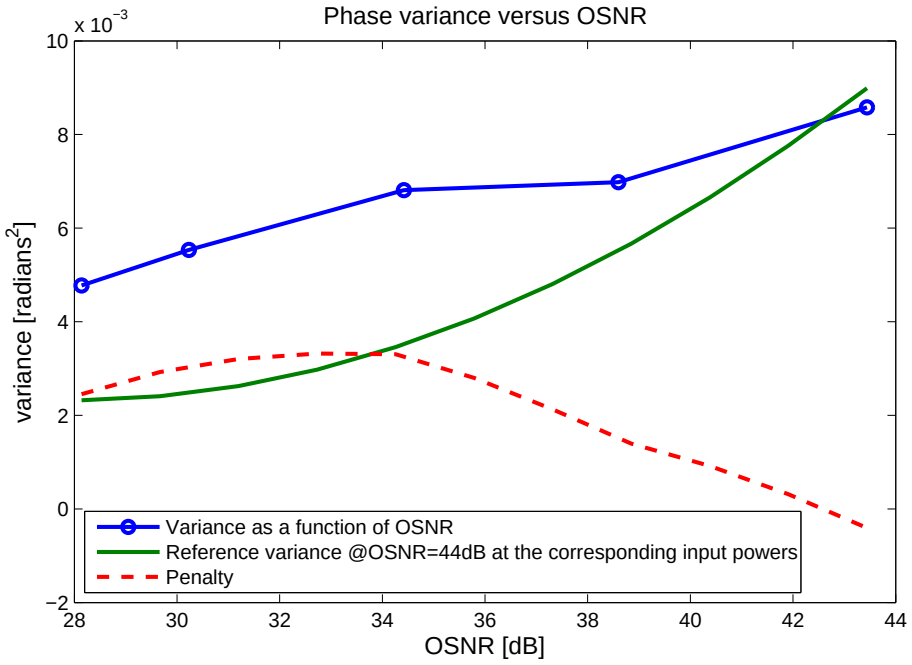

Figure 19: Phase variance as a function of OSNR, together with reference curve interpolated from figure 17 for the different injection ratios. The penalty is defined as additional phase variance over reference.

The results show that in the measured range the maximum penalty is a doubling of the variance compared to OSNR of 44 dB. The fact of negative penalty occurring in the tail at high OSNR is believed to be false, as the negative penalty falls within the measurement uncertainty.

In the measurement the master laser spectral peak power was kept constant and the, attenuation before, and the gain in the EDFA before the slave laser was changed. With increased gain the total ASE noise power and thereby the external injection ratio also increases. A reference, with a constant OSNR of 44 dB, was created to by interpolation of the results in figure 17, for the injection ratios used for comparison. The reference is needed since injection ratio alters with OSNR since noise loading of the system is used to alter the OSNR. The penalty was then defined as the measured variance after substraction by the reference.

Another aspect of keeping control of the laser detunings becomes evident by studying figure 20 where phase variance steeply increases near the edges of the locking bandwidth. The results gathered qualitatively and quantitatively agree well with the theoretical work of Bordonalli et al. [20].

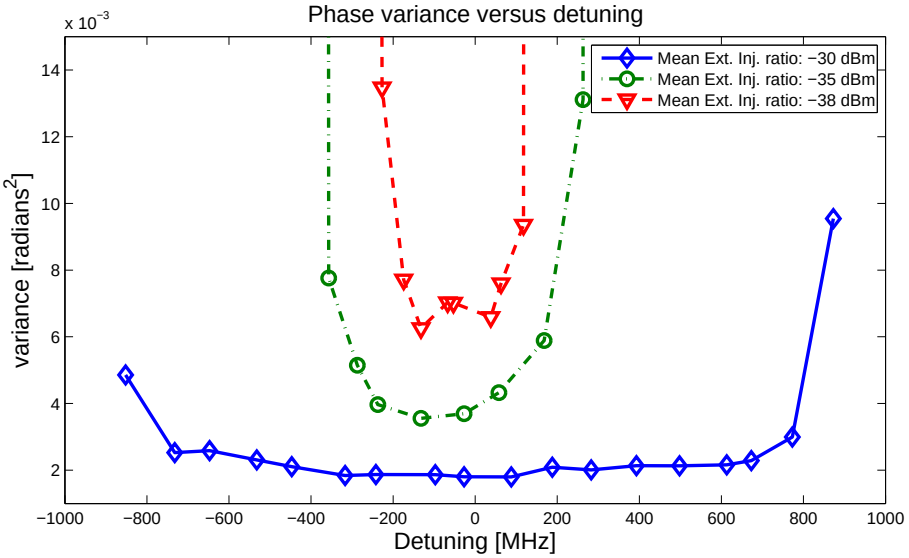

Figure 20: Phase variance as a function of detuning over the locking-bandwidth for three different external injection ratios.

The results in figure 20 shows how the phase variance peak at the edges of the locking-bandwidth. The bandwidth with approximately the same variance gets smaller swiftly when moving towards lower injection ratios.

8.3 Modulation Effects on Phase-Locking Performance

As suggested by Pezeshki et al. [24], active control of the detuning of the injection-locked system, while being in a locked state, as explained in section 5, can be done using dithering tones. The amplitude dithering tone impact at phase tracking performance was measured by driving the MZM at different different modulation depths. Figure 21 shows how different external injection ratios and different modulation depths affect phase variance. The measurements were conducted while driving the MZM with a 10 MHz sine tone.

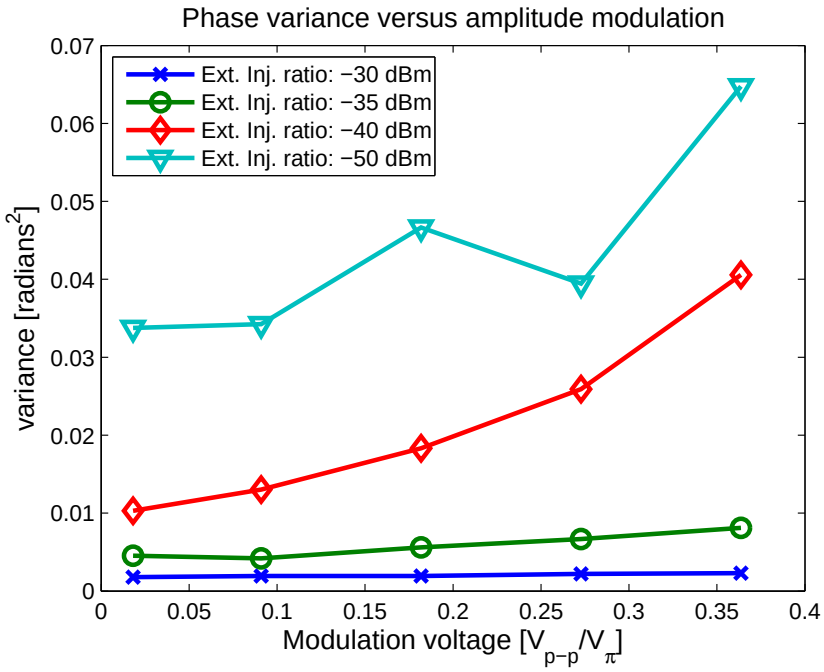

Figure 21: Phase variance at different locked states as a function of modulation depth for four different external injection ratios.

The results clearly shows an increased sensitivity to amplitude modulation with smaller injection ratios. The AM-to-PM transfer is significantly affecting the system at lower injection ratios and deeper modulation depths. The different phase variance levels at small modulation depths agree well with previous results.

In order to give a performance measure on modulation stripping ability, presented in figure 22, over and outside the locking bandwidth the MZM was replaced with a phase modulator manufactured by Lucent. The measurements were taken at two different injection ratios that would yield locking bandwidths well below 990 MHz which is the limit of the waveform generator used. The phase modulator were fed with a sinusoidal signal at two different modulation depths, -20 dBm and -27 dBm output to a RF-amplifier, -27 called small modulation depth and -20 dBm called moderate modulation depth in figure 22. The measurement were repeated for two different external injection ratios in order to investigate if it had any effect on the PM-to-PM transfer in the injection-locked system.

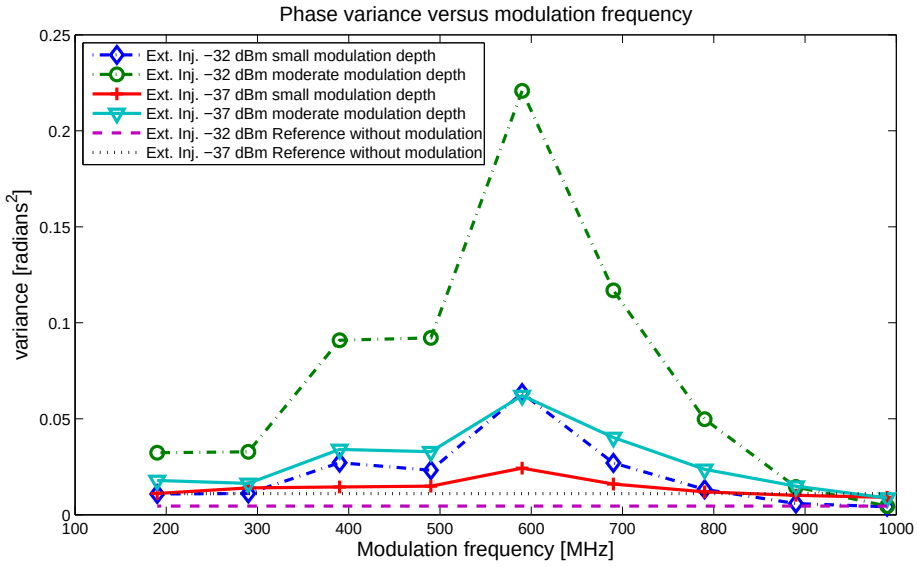

Figure 22: Phase variance at different locked states and modulation depths as a function of modulation frequency, while keeping the detuning close to zero.

These are results that can be observed as unexpected since the results from figure 14 suggests that the peak at 600 MHz should be outside the locking bandwidth for the lower injection ratio. It is also intriguing to observe the highly unequal phase variance response over the measured frequency span. The dramatic increase in variance can maybe partly be explained by previous results presented in figure 20. By modulation close to the edge of the locking-bandwidth, effectively providing an sideband coinciding with the locking-

bandwidth edge, phase variances seem to rise most significantly.

The peak at 600 MHz seem to be a system resonance, in the resolution the measurement was done the resonance does not seem to shift in frequency.

The high dependence on the external injection ratio is very interesting, according to these results 5 dB difference in injected power could be the difference between acceptable performance and inadequate phase tracking.

Caution is advised since the sine modulation poorly resemble the spectra obtained by modulating with BPSK and QPSK modulation formats. The results should not therefore be treated as fully valid for any other case than the case measured. The sensitivity to narrowband modulation close to the locking-bandwidth edge is however according to this experiment very significant.

These results suggest that a simple passband/stopband model of PM-to-PM transfer in injection locked systems may be an inadequate description, when narrowband modulation is used.

8.4 RIN Measurements

Another aspect in carrier recovery is to be able to regenerate a degenerated master from poor OSNR and thereby also poor RIN. As seen in the measurement setup, figure 10, the master laser is amplified twice before getting injected into the slave laser. This amplification makes the RIN performance of the master laser limited by amplified stimulated emission(ASE) from the EDFA:s, at a very high level.

For carrier recovery a RIN measurement was conducted in order to see which kind of improvements that could be observed. The RIN was measured on the master laser and the slave laser individually at on a frequency span of 1600 MHz, supported by the measurement system. The measurements were conducted by utilizing the taps used for power meters in the measurement setup in figure 10. Furthermore, the RIN measurement was done by connecting a measurement system which is shown in figure 23.

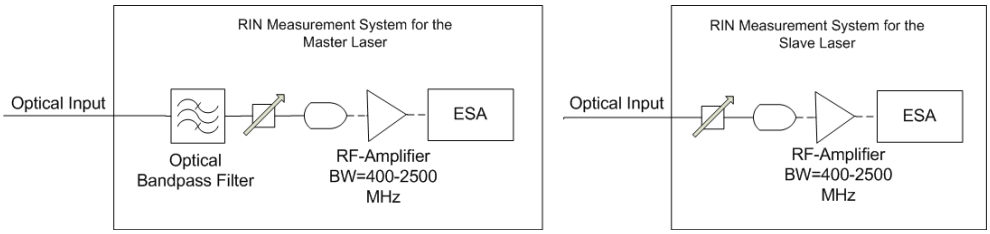

Figure 23: Measurement systems used for measuring the master laser and slave laser RIN respectively, the bandwidth of the optical filter is 0.8 nm.

The attenuator was set in such a way that the photo-current from the photodetector was constant between the measurement points. When measuring the RIN of the ASE-noise limited master laser an optical filter,with a bandwidth of 0.8 nm, was also employed to suppress the ASE signal-spontaneous beat noise.

The RIN measurements, in figure 24, shows that the RIN can be improved beyond the native master laser and slave laser RIN on measured frequencies. These results are inline with previous research conducted by Yabre et al. [26], which describes how the relaxation oscillation frequency is pushed towards higher frequencies, when the slave laser is injection-locked. The relaxation

oscillation frequency shift increases with external injection ratio, decreasing the RIN at measured frequencies.

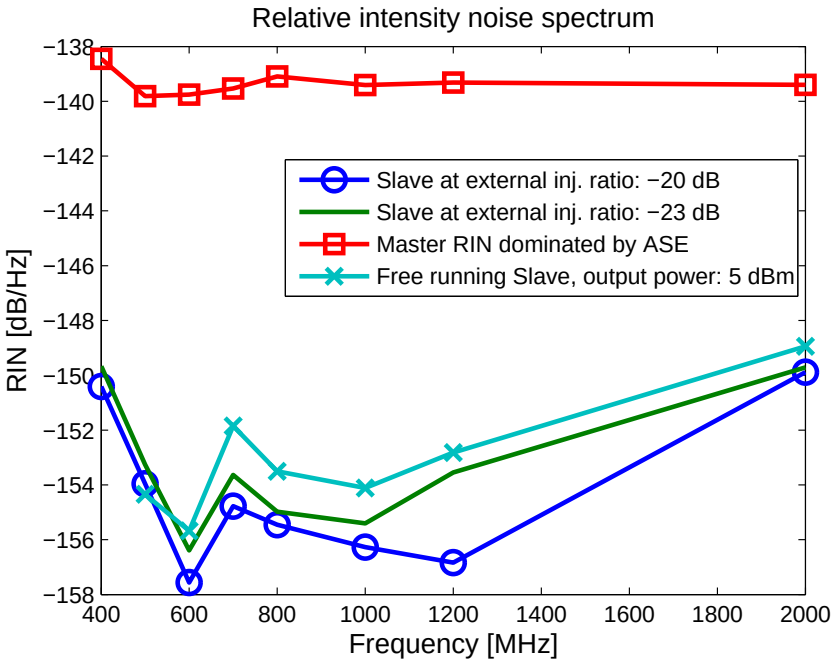

Figure 24: RIN measurements on the injected master dominated by ASE, plotted with RIN of the output slave laser, both unlocked and for two different external injection ratios

The RIN properties of the injection-locked system show that it is possible to improve the RIN spectrum of the recovered carrier significantly.

9 Discussion

The coherent measurements of injection-locked systems described in this thesis, add a new perspective to injection-locking, since time domain measurements are possible, effectively making analysis methods based on statistics feasible. Also spectral analysis is possible after coherent detections such as linewidth calculations as done by Duthel et al. in [25]. Amongst the advantages is the possibility to directly find phase variance which is the foundation of the measured results.

The threshold in sensitivity can maybe further be lowered by matching the pathlengths in both the signal and the LO arms of the measurement system. Also by using a master laser with narrower linewidth than the Santec TSL-210 additional sensitivity could be gained.

The extension of the studies has been lowered by the fact of the isolation of the slave laser used practically limits the external injection ratios to a maximum -30 dB. Having an unisolated slave laser would increased the dynamic range of those measurements by approximately between 30-40 dB. The uncertainty in the amount of optical isolation also makes absolute comparisons of the results to other studies difficult. However qualitative results are found and agrees with theory, especially the phase variance versus detuning relations found in 20 and in the work by Bordonalli et al. [20].

The measurements produced by the designed measurement system has shown that there are a series of interesting tradeoffs. Tradeoffs to be done in order to make injection-locked subsystems work optimally in conjunction to PSA applications. The largest tradeoff is the one suggested from the PM-to-PM transfer measurements and the external injection ratio versus phase variance measurements. A too large injection ratio would transfer more PM to the slave laser output while a too small injection ratio would degenerate the quality of the lock and generate excess phase noise.

A low injection ratio would also make the system less resilient towards AM-to-PM transfer, as shown in figure 21, making the decision of how much light that should be injected even more complex.

Another problem is the long and short term laser drifts that has to minimized in order to realize systems based on injection-locking, highly visible in the results of phase variance as a function of detuning, shown in figure 20. Moving

to small injection ratios increases the need for active control like the one described in section 5 as the locking bandwidth scales with injection ratio.

The measurements done on the variance dependence on phase modulation, shows unexpected results around 600 MHz in figure 22, this might be to some extrinsic frequency sensitivity in system. Another tentative explanation for this behavior can be the coincidence between sharp optical sidebands from the modulation and the edge of the locking-bandwidth. Figure 20 shows extreme increases in phase variance when system is detuned to the locking-bandwidth edge which could be a part of the explanation.

The results of the OSNR study in figure 19 are expected if disregarding the rolloff of the penalty towards low OSNR. Intuitively the penalty should increase with decreasing OSNR, however is the rolloff is in comparison to the measurement limits, and might not be actual. The fact that relatively few measurement points is used in interpolation induce errors, which weakens the possibilities to draw conclusions. Furthermore, the results show that there are an non-negligible penalty reducing OSNR.

10 Conclusions

This master thesis has aimed for introducing coherent measurements and developing an optical test setup for the studies of injection-locking, which has been achieved. The theoretical parts of the thesis thoroughly describes the injection-locking process together with a partial description of the phase noise generated in injection-locked systems. Amongst the conclusions that can be drawn is the well working concept of coherent measurements using the proposed optical setups. The sensitivity is high enough to measure phase variances down to the mrad^2 scale, which is anticipated to increase even further by path length matching. The accuracy of the method used is estimated to be ± 0.6 mrad^2.

The measurement setup dynamic range in terms of external injection ratio would be increased greatly by having optically unisolated lasers, eliminating the need of any EDFA:s in the system. Increasing flexibility of the setup and comparability of the results and thereby relevance.

Several tradeoffs has been identified, especially between PM-to-PM transfer and AM-to-PM transfer in terms of injection ratio to minimize the resulting phase variance of the total system. This is interesting since the scheme for active control of detuning, presented in section 5, involves amplitude dithering. Amplitude modulation together with the residual phase modulation from a carrier recovery scheme, makes the tradeoff between suppressing PM-to-PM and AM-to-PM more challenging.

There also exist a tradeoff between PM-to-PM transfer phase noise generated by a low injection-ratio. To little injected light would generate intrinsic phase noise according to the results in figure 17, where a to high injection ratio would increase the locking-bandwidth and also the PM-to-PM transfer according to figure 22.

In order to have long term system stability of injection locked systems with small locking bandwidths, active control is necessary if laser drift is not very well below the locking bandwidth.

The amplidtude modulation stripping capabilities of is dependent of the injection ratio as anticipated by Lau et al. [2]. Furthermore, extreme variance increases is believed to be induced by phase modulation by sine tones close to the locking-bandwidth.

The RIN performance has been measured to improve significantly by injection locking by injecting a master laser with poor RIN characteristics, ending up with slightly improved RIN performance over the unlocked slave laser at low frequencies.

There exists a penalty to lowering the OSNR of the light used to injection-lock the slave laser with in terms of phase variance.

11 Further research

In order to shed further light on the usability of more theoretical work needs to be conducted to put demands on the injection-locking process when used with PSA related applications. The demands put on the phase matching would together with the results and methods presented in this thesis give an overview, on the demands to be put on lasers and injection ratios. All this to balance tradeoffs against each other in a controlled manner.

The interesting results regarding phase modulation transfer also remain unexplained. Furthermore, the as the injection-locked laser applications are focused towards carrier regeneration, further studies of phase modulation transfer should be a prioritized topic. Especially repeating the sine modulation experiments with another slave laser to see if its repeatable. Also high speed BPSK and DPSK modulation, as done by Parmigiani et al, [22], could be used for further evaluation of the modulation stripping abilities of injection-locked systems.

Improvements in the setup is anticipated by the use of unisolated lasers, and also by path length matching and moving towards APC contacted or fully spliced setups.

As the locking bandwidth measurements did scale according to theory it might be interesting to repeat those measurements for unisolated lasers, to investigate if the result might be due a thermal effect.

During the course of the project the idea of cascaded injection-locked lasers were discussed several times. A cascaded injection-locked solution is schematically represented in figure 25, where a master laser is used to injection-lock slave laser 1 which in turn is used to injection-lock slave laser 2.

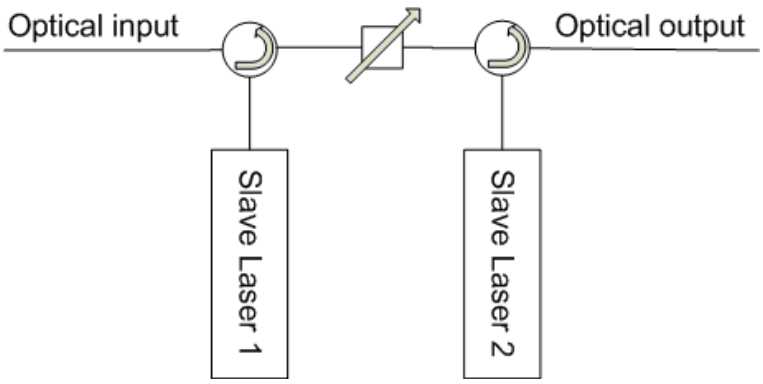

Figure 25: Two cascaded injection-locked lasers, where slave laser 1 is injection-locked to the optical input and slave laser 2 is locked to the output of slave laser 1.

A cascaded solution is anticipated to have several advantages since they can be biased ad different injection ratios and split up the problem of carrier recovery. The most evident scheme would be in the case of a signal that is both severely affected by amplitude noise and phase noise or modulation. The slave laser 1 could then be injection-locked at a high injection ratio allowing efficient suppression of AM-to-PM transfer while AM-to-AM transfer also is suppressed to a certain degree. Slave laser 2 would then be left with the PM-to-PM transfer which could be solved by having a low injection ratio suppressing the PM-to-PM transfer. Since amplitude modulation already is suppressed, very small amounts of AM-to-PM is anticipated to transfer through the cascade.

Also, for stripping amplitude modulation without transfer excessive phase noise, a two step injection-locked solution can be beneficial. Since the total desired suppression can be divided amongst the two steps. Both of them can allow a higher injection ratio, increasing the MTR but suppressing the AM-to-PM transfer.

References

[1] H. Stover and W. Steier, "Locking of laser oscillators by light injection," *Applied Physics Letters*, 1966.

[2] E. K. Lau, *High-Speed Modulation of Optical Injection-Locked Semiconductor Lasers*. PhD thesis, EECS Department, University of California, Berkeley, Dec 2006.

[3] J. Hansryd, P. Andrekson, M. Westlund, J. Li, and P. Hedekvist, "Fiber-based optical parametric amplifiers and their applications," *IEEE Journal of Selected Topics in Quantum Electronics*, vol. 8, no. 3, pp. 506–520, 2002.

[4] Y. Yamamoto, S. Machida, S. Saito, N. Imoto, T. Yanagawa, M. Kitagawa, and G. Bjork, "Quantum mechanical limit in optical precision measurement and communication," *Progress in optics*, vol. 28, no. 87, 1990.

[5] J. Levenson, I. Abram, T. Rivera, and P. Grangier, "Reduction of quantum noise in optical parametric amplification," *Journal of the Optical Society of America B*, vol. 10, no. 11, pp. 2233–2238, 1993.

[6] T. Simpson, J. Liu, and A. Gavrielides, "Bandwidth enhancement and broadband noise reduction in injection-locked semiconductor lasers," July 13 1999. US Patent 5,923,687.

[7] K. Iwashita and K. Nakagawa, "Suppression of mode partition noise by laser diode light injection," *IEEE Journal of Quantum Electronics*, vol. 18, no. 10, pp. 1669–1674, 1982.

[8] L. Chrostowski, C. Chang, and C. Chang-Hasnain, "Reduction of relative intensity noise and improvement of spur-free dynamic range of an injection locked VCSEL," in *Lasers and Electro-Optics Society, 2003. LEOS 2003. The 16th Annual Meeting of the IEEE*, vol. 2, 2003.

[9] J. Liu, H. Chen, X. Meng, and T. Simpson, "Modulation bandwidth, noise, and stability of a semiconductor lasersubject to strong injection locking," *IEEE Photonics Technology Letters*, vol. 9, no. 10, pp. 1325–1327, 1997.

[10] C. Lin and F. Mengel, "Reduction of frequency chirping and dynamic linewidth in high-speed directly modulated semiconductor lasers by injection locking," *Electronics Letters*, vol. 20, p. 1073, 1984.

[11] A. Pikovsky, M. Rosenblum, J. Kurths, and R. Hilborn, "Synchronization: A universal concept in nonlinear science," *American Journal of Physics*, vol. 70, p. 655, 2002.

[12] R. Adler, "A study of locking phenomena in oscillators," *Proceedings of the IRE*, vol. 34, no. 6, pp. 351–357, 1946.

[13] R. Pantell, "The laser oscillator with an external signal," *Proceedings of the IEEE*, vol. 53, no. 5, pp. 474–477, 1965.

[14] C. Henry, N. Olsson, and N. Dutta, "Locking range and stability of injection locked 1.54 μm InGaAsP semiconductor lasers," *IEEE Journal of Quantum Electronics*, vol. 21, no. 8, pp. 1152–1156, 1985.

[15] A. Murakami, K. Kawashima, and K. Atsuki, "Cavity resonance shift and bandwidth enhancement in semiconductor lasers with strong light injection," *IEEE Journal of Quantum Electronics*, vol. 39, no. 10, pp. 1196–1204, 2003.

[16] R. Lang, "Injection locking properties of a semiconductor laser," *IEEE Journal of Quantum Electronics*, vol. 18, no. 6, pp. 976–983, 1982.

[17] F. Mogensen, H. Olesen, and G. Jacobsen, "Locking conditions and stability properties for a semiconductor laser with external light injection," *IEEE Journal of Quantum Electronics*, vol. 21, no. 7, pp. 784–793, 1985.

[18] T. Simpson, J. Liu, A. Gavrielides, V. Kovanis, and P. Alsing, "Period-doubling route to chaos in a semiconductor laser subject to optical injection," *Applied Physics Letters*, vol. 64, p. 3539, 1994.

[19] A. Hurwitz, "On the conditions under which an equation has only roots with negative real parts," *Selected Papers on Mathematical Trends in Control Theory*, 1964.

[20] A. Bordonalli, C. Walton, and A. Seeds, "High-performance phase locking of wide linewidth semiconductor lasers by combined use of optical injection locking and optical phase-lock loop," *Journal of Lightwave Technology*, vol. 17, no. 2, p. 328, 1999.

[21] R. Weerasuriya, S. Sygletos, S. K. Ibrahim, R. Phelan, J. O'Carroll, B. Kelly, J. O'Gorman, and A. D. Ellis, "Generation of frequency symmetric signals from a bpsk input for phase sensitive amplification," in *Postdeadline papers*, (San Diego CA, USA), Optical Fiber Communications Conference (OFC), march 2010.

[22] F. Parmigiani, R. Slavík, J. Kakande, C. Lundström, M. Sjödin, P. Andrekson, R. Weerasuriya, S. Sygletos, A. D. Ellis, L. Grüner-Nielsen, D. Jakobsen, S. Herstrom, R. Phelan, J. O'Gorman, A. Bogris, D. Syvridis, S. Dasgupta, P. Petropoulos, and D. J. Richardson, "All-optical phase regeneration of 40gbit/s dpsk signals in a black-box phase sensitive amplifier," in *Postdeadline papers*, (San Diego CA, USA), Optical Fiber Communications Conference (OFC), march 2010.

[23] G. Lu and T. Miyazaki, "Optical Phase Add–Drop for Format Conversion Between DQPSK and DPSK and its Application in Optical Label Switching Systems," *IEEE Photonics Technology Letters*, vol. 21, no. 5, pp. 322–324, 2009.

[24] J. Pezeshki, M. Saylors, H. Mandelberg, and J. Goldhar, "Generation of a CW local oscillator signal using a stabilized injection locked semiconductor laser," *Journal of Lightwave Technology*, vol. 26, no. 5, pp. 588–599, 2008.

[25] T. Duthel, G. Clarici, C. Fludger, J. Geyer, C. Schulien, and S. Wiese, "Laser Linewidth Estimation by Means of Coherent Detection," *IEEE Photonics Technology Letters*, vol. 21, p. 20, 2009.

[26] G. Yabre, H. De Waardt, H. van den Boom, and G.-D. Khoe, "Noise characteristics of single-mode semiconductor lasers under external light injection," *Quantum Electronics, IEEE Journal of*, vol. 36, pp. 385 –393, mar 2000.